More Fundamentals of Dilute Suspension Collapse and Choking for Vertical Conveying Systems

Guangwen Xu, Kousuke Nomura, Shiqiu Gao, and Kunio Kato
Dept. of Biological and Chemical Engineering, Gunma University, Kiryu, Gunma 376-8515, Japan

Using gas-solid flows in circulating fluidized-bed risers to analogize vertical pneumatic conveying systems, the collapse of dilute suspension, that is, the choking of accumulative type, was studied in three different risers with respect to different particles. The collapse of dilute suspension was dominated by an identical differential pressure drop over the measuring section. This differential pressure drop was independent of gas velocity and riser diameter, but varied with particle properties. The saturation carrying capacity, the solid flow rate at the dilute suspension collapse, was closely related to particle characteristics and riser diameter. With an increase in the riser diameter, it increased for lighter and smaller particles, but decreased for heavier and larger particles. Based on these experimental measurements, as well as the related literature reports, a correlation was developed for the saturation carrying capacity by analyzing its dependencies on gas velocity and riser diameter. More than 150 experimental data of the saturation carrying capacity available in the literature were compiled to evaluate the accuracy of the proposed correlation by comparing with 13 other literature correlations, demonstrating that this new method has the highest accuracy.

Introduction

For vertical concurrent gas-solid flows, such as that in circulating fluidized-bed (CFB) risers, the term "choking" has generally been used to describe a particular change in flow behaviors when a pneumatic conveying flow collapses into a relatively dense condition. Here, the pneumatic conveying flow refers to the lean-phase operation with little axial variation in flow characteristics and is also called dilute suspension or sometimes dilute transport (Yerushalmi and Cankurt, 1979; Schnitzlein and Weinstein, 1988). Owing to the importance of choking for the design of transport lines and dense reactors, a great deal of work has been conducted to understand the phenomenon and to quantify its occurrence. Nevertheless, the definition of choking remained unclear until three different mechanisms that trigger the choking were distinguished by Bi et al. (1993). Of the three types of choking defined by them, only the so-called accumulative choking (type A) and classical choking (type C) are due to the inherent changes in gas-solid flow itself, while the type B choking actually stems from facility inefficiency. The accumulative choking stresses the essence of solid accumulation at the bottom of a vertical conveying tube and concerns little whether the process is stepwise or progressive, although both have been reported in the literature. In comparison, the prominent characteristics of type C choking is said to be the sudden formation of slugs or plugs when a steady operation ceases. Matsen (1982) and Chong and Leung (1986) have also accentuated that the choking phenomenon essentially denotes an abrupt or rapid transition of a gas-solid flow from dilute to dense, even though different flow structures possibly prevail at this transition.

Without distinguishing the different types of choking, the vertical concurrent gas-solid flows were classified into choking and nonchoking systems (Yousfi and Gau, 1974; Yang, 1976; Smith, 1978; Leung, 1980a,b; Konrad, 1986). This distinction was based on the first choking definition of Zenz (1949) and Zenz and Othmer (1960), and was proposed to account for the experimental finding that slugging/plugging did not always occur when a lean-phase conveying flow was terminated. Under certain conditions, the flow was found to

Correspondence concerning this article should be addressed to K. Kato.

progressively become denser and less uniform, with the formation of particle clusters/streams and the onset of considerable internal solid recirculation (Capes and Nakamura, 1973; Leung and Wiles, 1976; Yerushalmi and Cankurt, 1979). By defining the accumulative choking, the choking phenomenon should then prevail in all vertical pneumatic conveying systems. Either the type A (for nonslugging system) or type C (for slugging system) choking must become pronounced when a lean-phase flow collapses, depending on the flow conditions such as column diameter, solid density, particle size and the experimental technique for finely adjusting the gas/solid supply (Nomura, 1998).

On the other hand, the gas-solid flows in CFB risers possess different flow regimes. With reducing gas velocity at a given solid flow rate, they are, in succession, dilute suspension, fast fluidization, turbulent fluidization, bubbling fluidization, incipient fluidization, and fixed bed (Li and Kwauk, 1994; Kwauk and Li, 1996), respectively. Hence, the choking at dilute suspension collapse must be the type A choking, and the type C choking cannot come into play until the flow transits to bubbling fluidization. This implies that the type A choking corresponds to the regime transition from dilute suspension to fast fluidization, as was similarly suggested by Matsen (1982), Yang (1984), and Chong and Leung (1986). Two choking points are also possible for one system (Bi et al., 1993; Bai et al., 1998), with the type A choking having a smaller solid flow rate for a specified gas velocity or a higher choking velocity for a given solid flow rate. Nonetheless, the type C choking is essentially condition-dependent and predominant only for those systems with small column diameters (Nomura, 1998; Xu et al., 1999a). For most practical gas-solid conveying systems, the predominant choking should be type A since such flows are usually free of slugs/plugs. Gas bubbles, as well as their induced dynamics, can be similarly observed, but the relevant hydrodynamic features would be commonly recognized as a regime transition other than a choking of type C. Therefore, the commonly encountered choking should be the accumulative type exclusively that occurs just as a dilute suspension collapse.

This study concerns the mechanics and quantification of the accumulative choking. After a review of the literature work, experiments were conducted to observe the mechanism dominating the dilute suspension collapse and the type A choking, with an emphasis on the influences of the column diameter. Then, a correlation was developed for the solid flow rate at the choking, and was validated by comparing with the literature measurements. From the viewpoint of solid conveying, this solid flow rate just corresponds to the maximal attainable value for a given gas velocity, called the choking velocity U_{ck}, without solid accumulation at the bottom of the conveying column. Therefore, it is generally the same as the saturation carrying capacity G_s^* of the gas velocity employed (Zenz and Weil, 1958; Wen and Chen, 1982; Yang, 1983; Li et al., 1992).

Existing Work

Table 1 summarizes the well-documented literature correlations for U_{ck} and G_s^*, along with their corresponding fundamentals (assumptions) used for correlation development. Of the correlations, only the recent one from Xu et al. (1999b) clearly mentioned that it was for type A choking, while the others did not consider the differences in choking definition. The correlation of Leung et al. (1971) was based on the assumption that the gas-particle slip velocity at choking is equal to the free-fall (terminal) velocity u_t of a single particle and that the voidage at choking ϵ_{ck} is equal to 0.97. Yousfi and Gau (1974) suggested that choking occurs when a vertical uniform suspension flow becomes unstable, which was thought to be related to the Froude number Fr at the choking velocity U_{ck}. On account of the serious deviation stemming from the assumption by $\epsilon_{ck} = 0.97$ of Leung et al. (1971), Yang (1975) assumed a constant friction coefficient of 0.01 of solids to the tube wall at choking [computed from Hariu and Molstad (1949)]. It was considered that choking takes place when the solids-to-wall friction is overcome by the solid weight. The gas-solid slip velocity at choking was also set as the particle terminal velocity u_t in the equation of Yang (1975). For correlating the high-pressure choking data of Knowlton and Bachovchin (1975), Punmani et al. (1976) modified the equation of Yang (1975) by applying a factor to the solids-to-wall friction coefficient. Based on a plot of slip velocity versus gas velocity produced by Matsen (1982), Chong and Leung (1986) derived an explicit equation for the choking velocity as well. In 1983, Yang further analyzed the solids-to-wall friction and found that the friction factor of 0.01 was accurate only for nonslugging situation and another factor of 0.04 must be adopted for slugging systems, which led to an improved equation for G_s^*. The correlation of Day et al. (1990) was developed by assuming that choking occurs at the solid inlet of the transport line when a particularly defined parameter becomes zero. Later, Bi et al. (1993) pointed out that the zero value of such a parameter denoted essentially the onset of axial variation. The equations of Day et al. (1990) were presented in two different forms for monodisperse and polydisperse particles, respectively. The correlations of Knowlton and Bachovchin (1975), Mink (1983), Bi and Fan (1991), and Bai and Kato (1995) are purely empirical, while that of Xu et al. (1999b) is based on experimentally observed dependencies of G_s^* upon U_{ck} and D_t.

A few other correlations have also been reported. Based on the authors' own experimental data, Zenz and Othmer (1960) and Doig and Roper (1963) correlated the Froude number with the mass-flow rate ratio of particles to gas. However, due to their low accuracy, these two correlations have not been popularly noted by the academic circles (Leung et al., 1971). Models and methods were also developed by Leung and Wiles (1976) and by Briens and Bergougnou (1985, 1986) to calculate the choking parameters of multisized particle systems. For validation, all of the correlations used the measurements of Knowlton and Bachovchin (1975), the only data available for polydisperse particles. The correlation of Yang (1975) was extended to the case of multisized particles by Leung and Wiles (1976) and by Briens and Bergougnou (1985), while the model of Briens and Bergougnou (1986) assumed that choking occurs when the annular zone grows to occupy 25% of the total pipe cross-sectional area. Nonetheless, the choice of 25% was considered arbitrary and did not correspond to any variational condition related to choking and dilute suspension collapse (Bi et al., 1993). A theoretical criterion has been proposed by Li et al. (1992) to judge the occurrence of choking corresponding to the dilute suspension collapse on the basis of the so-called energy-minimization

Table 1. Correlations for Choking Prediction Available in the Literature

No.	Reference	Equations	Fundamental or Assumption
C1	Leung et al. (1971)	$U_{ck} = 32.3\dfrac{G_s}{\rho_p} + 0.97u_t$	$\epsilon_{ck} = 0.97$ and gas-solid slip velocity is u_t
C2	Yousfi and Gau (1974)	$\dfrac{U_{ck}}{\sqrt{gd_p}} = 32\,Re_t^{-0.06}\left(\dfrac{G_s^*}{\rho_f U_{ck}}\right)^{0.28}$	Empirical correlation by suggesting that the dilute suspension flow is dependent on Froude number.
C3	Yang (1975)	$G_s^* = (U_{ck}/\epsilon_{ck} - u_t)(1-\epsilon_{ck})\rho_p$ $\dfrac{2gD_t(\epsilon_{ck}^{-4.7}-1)}{(U_{ck}/\epsilon_{ck}-u_t)^2} = 0.01$	Choking occurs when solid weight overcomes the solids to wall friction that is assumed to be 0.01. Gas-solid slip velocity is set as u_t.
C4	Punwani et al. (1976)	$\dfrac{2gD_t(\epsilon_{ck}^{-4.7}-1)}{(U_{ck}/\epsilon_{ck}-u_t)^2} = 0.008743\rho_f^{0.77}$	Improving Yang (1975) by formulating the solids to wall friction.
C5	Knowlton and Bachovchin (1975)	$\dfrac{U_{ck}}{\sqrt{gd_p}} = 9.07\left(\dfrac{\rho_p}{\rho_f}\right)^a\left(\dfrac{G_s^* d_p}{\mu_f}\right)^b\left(\dfrac{d_p}{D_t}\right)^c$ $a = 0.347,\ b = 0.214,\ c = 0.246$	Pure empirical correlation by correlating their data measured at high pressure.
C6	Matsen (1982)	$U_{ck} = 10.74u_t\left(\dfrac{G_s^*}{\rho_p}\right)^{0.227}$	Based on Matsen's slip velocity-voidage relationship. Chong and Leung (1986) derived the equation.
C7	Yang (1983)	$\dfrac{2gD_1(\epsilon_{ck}^{-4.7}-1)}{(U_{ck}/\epsilon_{ck}-u_t)^2} = 681{,}000\left(\dfrac{\rho_f}{\rho_p}\right)^{2.2}$	Improving Yang (1975) by formulating the solids to wall friction.
C8	Mink (1983) (format modified)	$\dfrac{201.6gd_p}{U_{ck}^2} = \left[\dfrac{(1-\varphi)\rho_f\rho_w d_p}{\varphi(\rho_p-\rho_f)\rho_p D_t}\right]^{0.34}$	Pure empirical correlation. ρ_w, the density of water, $\varphi = G_s^*/(\rho_p U_{ck})$
C9	Day et al. (1990) (format compiled)	$\epsilon_0 = \dfrac{Ku_t}{U_{ck}}\cdot\dfrac{1}{1-\sqrt{\rho_f/\rho_p}}$ $K = \begin{cases} 1, & \text{for } d_p \ge 250\ \mu\text{m} \\ \dfrac{0.89\sqrt{gd_p(\rho_p-\rho_f)}}{u_t\rho_p^{0.5}}, & \\ & \text{For } d_p < 250\ \mu\text{m} \end{cases}$ $\dfrac{G_s^*}{U_{ck}\rho_p} = \dfrac{1-\epsilon_0}{\epsilon_0}\cdot\dfrac{1-\sqrt{\rho_f/\rho_p}}{\sqrt{\rho_p/\rho_f}-1}$	Based on an assumption that choking occurs at the inlet to the transport line (riser) when a particularly defined parameter becomes zero, which essentially implies the onset of axial variation (Bi et al., 1993). ϵ_0 refers to the radially averaged voidage at the inlet. This C9 was for monodisperse particles, and the C10 shown below was for polydisperse particles.
C10	Day et al. (1990)	$\epsilon_0^{3.2} = \dfrac{Ku_t}{U_{ck}}\cdot\dfrac{1}{1-\sqrt{\rho_f/\rho_p}}$	
C11	Bi and Fan (1991)	$\dfrac{U_{ck}}{\sqrt{gd_p}} = 21.6\,Ar^{0.105}\left(\dfrac{G_s^*}{\rho_f U_{ck}}\right)^{0.542}$	Purely empirical correlation similar to Yousfi and Gau (1974).
C12	Bai and Kato (1995)	$\dfrac{G_s^* d_p}{\mu} = \dfrac{1}{8}Fr^{1.85}Ar^{0.63}\left(\dfrac{\rho_p-\rho_f}{\rho_f}\right)^{-0.44}$	Purely empirical correlation by neglecting diameter influence.
C13	Xu et al. (1999b)	$\dfrac{G_s^*}{\rho_p\mu_t} = K\left(\dfrac{U_{ck}-u_t}{u_t}\right)^a\left(\dfrac{D_t}{d_p}\right)^b$ $a = 2.68 - 0.0037Ar$ $b = 2.13 - 0.53\ln Ar$ $K = \begin{cases} 0.0094(Ar/100)^{4.81}, & Ar \le 87 \\ 0.0087(Ar/100)^{4.17}, & Ar \ge 87 \end{cases}$	Empirical correlation based on experimentally observed dependencies of G_s^* on column (riser) diameter and gas velocity.
C14	This work	$a = 2.355 - 0.00191Ar$ $b = 1.740 - 0.441\ln Ar$ $K = \begin{cases} 0.0158(Ar/100)^{4.093}, & Ar \le 50 \\ 0.00923(Ar/100)^{3.344}, & Ar \ge 50 \end{cases}$	Improving Xu et al. (1999b) by relating the parameters a, b and K to literature G_s^* as well.

multiscale model (EMMS). However, complicated computation is needed to apply the criterion to actual computations (Xu and Li, 1998). The choking phenomenon was also analyzed with the minimum pressure drop across the whole column detected when reducing the gas velocity gradually at a specified solid flow rate (Capes and Nakamura, 1973). This, however, was not commonly acknowledged due to discrepancies in understanding the minimal pressure drop (Leung, 1980a,b; Matsumoto and Marakawa, 1987; Yerushalmi and Cankurt, 1979; Bi and Fan, 1991). In fact, such a pressure drop was not applied to the choking determination by Briens and Bergougnou (1986) and by Drahoš et al. (1988), although it was obviously observed in their experiments.

Extensive work has also been carried out to compare the various correlations and computation methods mentioned above. The earlier works include those by Punwani et al. (1976) and Leung (1980a,b). Although it is difficult to comment on the correlation accuracy that they gave (due to the limited data used for the validation), a suggestion made by Leung (1980a,b) is noteworthy. That is, any correlation without column diameter included should not be recommended for large-scale facilities. An evaluation was then made by Briens and Bergougnou (1986) for the correlations of Knowlton and Bachovchin (1975), Mink (1983), Yousfi and Gau (1974), Punwani et al. (1976), and Yang (1983). A total of 74 experimental points compiled from Zenz (1949), Lewis et al. (1949), Ormiston (1966), and Capes and Nakamura (1973) were employed. Through computing the relative deviations, they concluded that, for monosized particles, the equation of Yang (1983) gave the best predictions, whereas those of Knowlton and Bachovchin (1975) and Mink (1983) showed very poor accuracy. A method proposed in the same article for multisized particles was also shown to have better accuracy than any other model, such as those of Leung and Wiles (1976) and Briens and Bergougnou (1985). By including the measurement of Yerushalmi and Cankurt (1979) into the data set utilized by Briens and Bergougnou (1986), Chong and Leung (1986) compared the correlations of Leung et al. (1971), Yousfi and Gau (1974), Yang (1975, 1983), Punwani et al. (1976), and Matsen (1982). Attention was paid to the differences raised by different particle groups. It was found that the equation of Yousfi and Gau (1974) was applicable to groups A and B particles of Geldart's classification (Geldart, 1973) and that of Yang (1975, 1983) can be used for monosized group D particles. The use of the surface-to-volume mean diameter was suggested for multisized particles, showing that the correlation from Leung et al. (1971) gave a better prediction. Using the same set of data compiled by Briens and Bergougnou (1986), Day et al. (1990) stated that their correlation could give a slightly better result than that obtained by using the equation of Yang (1983) for single-sized particles. Using the data of Knowlton and Bachovchin (1975), they also showed that their equation for polydisperse particles was more accurate than the model of Briens and Bergougnou (1986) (the weight-average particle diameter was used). The latest comparison by Bi et al. (1993) stressed that it was certainly impossible to unify the choking data having different definitions using only one correlation. Accordingly, the literature data were classified into three groups in accordance with their criteria of choking determination. A total of 71 points for type A choking and 74 for type C choking were compiled, resulting in the equations of Yang (1975, 1983) and Bi and Fan (1991), which are recommended for the accumulative choking, while that of Yousfi and Gau (1974) is recommended for the classical choking.

In summary, we thus can see that the mechanics dominating the occurrence of choking is still not clear. Various assumptions have been proposed for correlation development, but none of them has been supported by evidence obtained from experiments. Another important issue related to choking and dilute suspension collapse is the diameter influence. In addition to a conceptual indication by Leung (1980a,b), Yang (1983) clearly showed that the choking in the vertical conveying system is greatly dependent on bed configuration, as well as on solid characteristics. The tube diameter has also been treated as a critical parameter by Chong and Leung (1986) in evaluating a choking correlation. However, so far, very few studies have been devoted to choking behaviors in conveying columns with different diameters, although phenomenal delineations for dilute suspension collapse in different CFB risers have been made by Yerushalmi and Avidan (1985) and by Chang and Louge (1992). Some correlations summarized in Table 1 involved the tube diameter D_t, and all of them actually resulted from mathematical regressions. With these recognitions, a series of works has recently been conducted to characterize the dilute suspension collapse and choking in different CFB risers (Xu et al., 1997a,b, 1999a) and to determine the influence of riser diameter on the saturation carrying capacity (Xu et al., 1999b, 2000). This article is an extension of such previous works, while a great effort is made to relate the present findings to those presented in the literature. More than 150 experimental data are compiled to evaluate the major correlations for choking predictions. Even now, there is confusion as to the accuracy of literature correlations and the choice of them. This stems not only from a poor understanding of the choking mechanics, but also from the insufficient validation of the literature equations. Before Bi et al. (1993), all comparisons did not consider the different types of choking, and only the experimental data before the 1970s were used for the comparison. The distinction of choking definitions enabled rather good estimations of various correlations, but many of the measurements reported in the last few decades were not included in the work of Bi et al. (1993). In addition, Bi et al. considered only seven of the correlations listed in Table 1.

Experimental Studies

Figure 1 shows the experimental CFB. The three risers used had the same bed height of 3.0 m, but different inner diameters of 66, 97 and 150 mm, respectively. A common downcomer that had an ID of 150 mm and a height of 1.0 m was employed to serve all of the risers. The gas velocity entering the riser U_g was measured using an orifice meter. The gas-flow rate to the downcomer and the downer bed height were constantly maintained throughout the experiments (the downer bed height referring to the height of the fluidized particles in the downcomer). Xu et al. (1999a) showed that the downer bed height actually has little influence on the measurement of the dilute suspension collapse. The solid circulation rate G_s was controlled using a ball valve and was

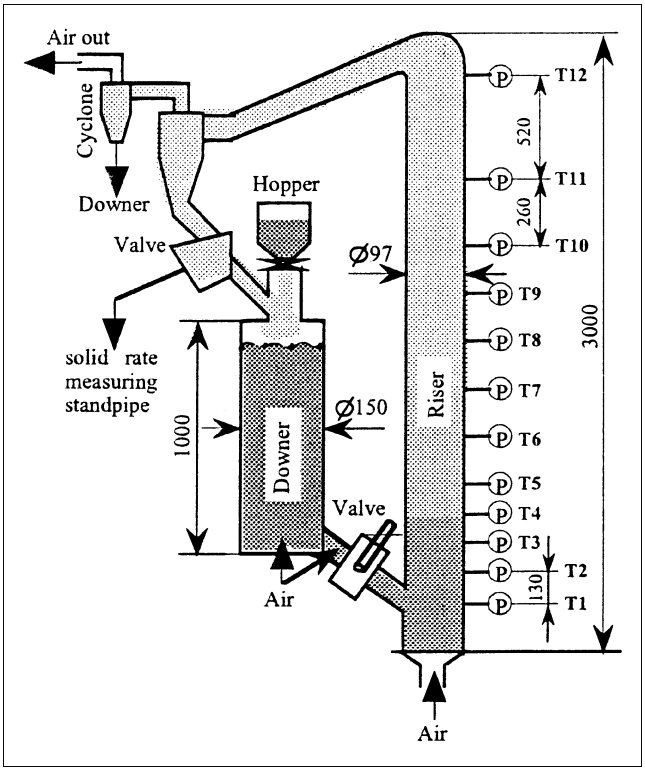

Figure 1. Experimental apparatus.

measured by diverting the circulating particles into a solid-rate-measuring standpipe within a period preset with a timer.

The dilute suspension collapse was judged with the differential pressure drop $\Delta P_d/\Delta Z$ measured between taps T1 and T2. In order to accurately detect the collapsing point, it was thought that the bed section selected for the measurement, for example, between taps T1 and T2, should be located as low as possible because the dense flow always appears first in the bottom region of the bed. In this study, the lowest tap T1 was located on the opposite side of the solid feed inlet connected to the downcomer, which was only 200 mm above the riser distributor. This also allowed the direct impact of the

Table 2. Properties of Particles Used in this Study

FCC-I (Group A)		FCC-II (Group A)		Alumina (Group A-B)		Silica Sand (Group B)	
d_{pi} (μm)	F_{pi} (%)	d_{pi} (μm)	F_{pi} (%)	d_{pi} (μm)	F_{pi} (%)	d_{pi} (μm)	F_{pi} (%)
137.5	100.0	125.0	99.2	210.0	95.5	460.0	100.0
115.5	99.6	105.0	97.5	177.0	78.2	385.0	99.8
98.0	95.1	88.0	95.2	149.0	28.8	300.0	99.2
82.5	78.3	75.0	92.5	125.0	12.4	213.5	95.3
69.0	68.2	63.0	72.5	105.0	8.8	163.0	51.3
58.0	49.4	53.0	46.3	88.0	6.6	127.5	30.5
49.0	37.9	45.0	16.7	75.0	5.6	97.0	4.2
41.5	15.4	38.0	7.7	63.0	3.7	81.0	2.1
30.0	6.6					63.5	0.8
ρ_p: 1,623 kg/m^3		ρ_p: 1,460 kg/m^3		ρ_p: 1,300 kg/m^3		ρ_p: 2,220 kg/m^3	
d_p: 65.0 μm		d_p: 54.2 μm		d_p: 145.4 μm		d_p: 166.0 μm	
Ar: 15.6		Ar: 8.1		Ar: 138.7		Ar: 355.5	
u_t: 0.193 m/s		u_t: 0.128 m/s		u_t: 0.574 m/s		u_t: 1.028 m/s	

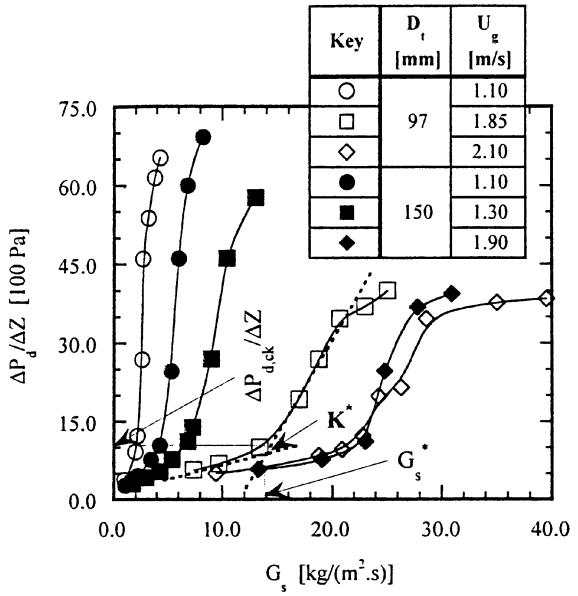

Figure 2. Pressure gradients at the bed bottom in different risers for FCC-I particles.

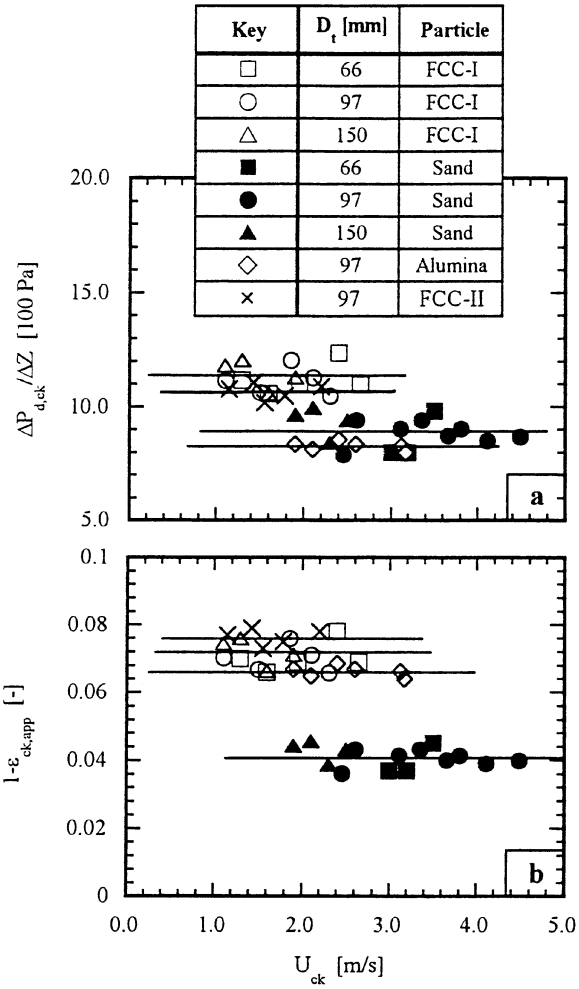

Figure 3. Critical differential pressure drop and apparent solid concentration dominating the dilute suspension collapse and choking.

solid feed on the pressure measurement to be avoided. The distance between taps T1 and T2 was set at 130 mm to ensure a minimal detectable pressure drop on the one hand and a maximal representation for the local flow on the other hand. The measuring height H_d was determined as the height above the riser distributor of the middle point of the measured bed section. An integrated pressure detector with a successive data acquisition system was used for the measurement of the differential pressure drop $\Delta P_d/\Delta Z$. The measuring range of the pressure detector was $0 \sim 1999$ mmH_2O, and 5,000 data points were collected in each sampling. In this study, the collapse of dilute suspension was measured at different solid circulation rates by varying the opening of the solid controlling valve at given superficial gas velocities.

The properties of all used particles are listed in Table 2, where the diameter d_p represents the surface-to-volume mean diameter and the groups of particles refer to the classification of Geldart (1973).

Mechanics

Figure 2 shows the typical differential pressure drops between taps T1 and T2, $\Delta P_d/\Delta Z$, around the dilute suspension collapse for particle FCC-1. It is clear that there were similar collapsing behaviors in both the risers employed. Under a specified gas velocity, the collapse is characterized by a rapid variation in the differential pressure drop $\Delta P_d/\Delta Z$ from insensitive to sensitive with respect to the change in solid circulation rate G_s. Accordingly, the critical point denoting the dilute suspension collapse can be definitely determined by the approach illustrated in Figure 2 (Xu et al., 1997a, 1999a). That is, two lines are used to approximate the variational curves before (dilute suspension) and after (rapid accumulation region) the collapse. Their intersection, marked as point K* in Figure 2, thus reasonably represents the termination of the dilute suspension flow. Starting from point K*, the axial profile of the cross-sectionally averaged voidage computed from the differential pressure drop also becomes axially nonuniform, as a result of the greatly increased pressure drop in the bed bottom region (Xu et al., 1997a, 1999a). Therefore, the determination approach shown here is essentially consistent with the definition of the accumulative choking. Further, one can find that the same physical meaning is also taken by a few other literature criteria demarcating the transition from lean-phase transport to fast fluidization such as those from Takeuchi et al. (1986) and Li et al. (1988). In a 10-m-high riser, Li et al. (1988) defined the transition as the beginning of a flow condition with a constant solid flow rate that is independent of the solid inventory in the whole CFB. This solid flow rate actually cannot come into play unless the dilute suspension flow is trigged into collapse.

With the determination method exemplified in Figure 2, the relevant critical parameters for dilute suspension collapse, namely, for the accumulative (type A) choking, can then be quantified from experimental measurements. As examples, Figure 2 shows the saturation carrying capacity G_s^* and the differential pressure drop $\Delta P_{d,ck}/\Delta Z$ determined using such an approach.

Summarized in Figure 3a are the critical differential pressure drops between taps T1 and T2, $\Delta P_{d,ck}/\Delta Z$, measured in three CFB risers for four different kinds of particles. It can be seen that an identical $\Delta P_{d,ck}/\Delta Z$ prevails at the dilute suspension collapse for a given species of particles (at least for groups A and B particles). This critical pressure drop is independent of gas velocity (U_g) and riser diameter (D_t), but varies with particle properties (d_p and ρ_p). For this study, the particle FCC-I had the highest $\Delta P_{d,ck}/\Delta Z$, while alumina took the lowest value.

Essentially, Figure 3a implies that the collapse of dilute suspension is dominated by a critical differential pressure drop across the measuring section. This finding has never been documented before, but can be identified with several literature measurements. In addition to the diagram of $\Delta P_d/\Delta Z$ vs. G_s plotted by Xu et al. (1999a) from the data of Rhodes and Geldart (1985) and of Yerushalmi and Cankurt (1979), Figure 4 shows the pressure drops $\Delta P_{d,ck}/\Delta Z$ determined from a few other literature measurements using the approach illustrated in Figure 2. The detailed measurement conditions can be found in Table 3. It is evident that the same result can be derived from Figure 4 for the mechanics dominating the dilute suspension collapse, although these literature measurements were obtained using different risers (D_t) and at different measuring heights (H_d). Nevertheless, the value of such a critical differential pressure drop differs from report to report, and these differences are thought to be mainly due to the different particles employed. In addi-

Key	Author(s)	H_d/H_t [m/m]	Particle
○	Hirama et. al.	3.0/5.5	FCC
▼	(1995)	6.0/10.0	FCC
■	Hirama et. al. (1992)	3.0/5.5	HA54
+	Yerushalmi	2.5/8.5	HFZ-20
◆	and Cankurt	2.5/8.5	FCC
□	(1979)	0.5/8.5	HFZ-20
●	This work	0.37/3.0	FCC-I
△		0.5/3.0	

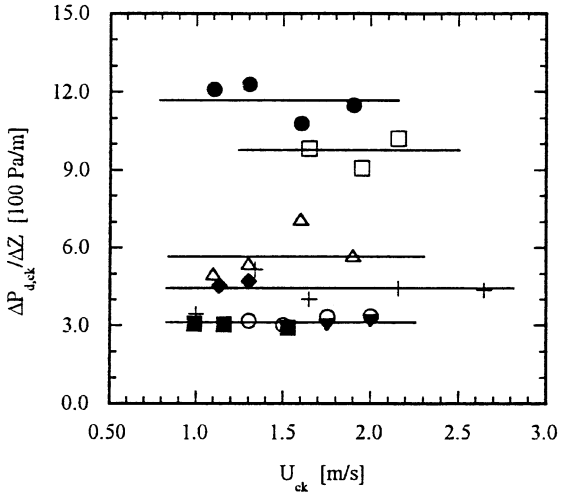

Figure 4. Identification of the critical differential pressure drop dominating the dilute suspension collapse and choking using literature data.

Table 3. Experimental Conditions of the Literature Data Referred to in this Article*

No.	Author(s)	D_t (mm)	Particle	Type†	d_p (μm)	ρ_p (kg/m^3)	Ar	u_t (m/s)	Choking Definition
			(a) *Accumulative choking*						
D1	This work	66	FCC-I	A	76	1,623	15.62	0.187	Sets D1 to D5 are defined according to Figure 2, and the choking for D6 and D7 refer to the onset of the rapid increase in solids concentration, that is, in differential pressure drop in the measuring section at the dilute suspension collapse.
		97	FCC-II	A	54	1,460	8.05	0.124	
		150	Alumina	A-B	145	1,300	140.0	0.573	
			Sand	B	166	2,220	355.9	1.023	
D2	Yerushalmi and Cankurt (1979)‡	152	HFZ-20	A	49	1,450	5.98	0.1045	
			FCC	A	49	1,070	4.41	0.0809	
D3	Hirama et al. (1992)	100	HA54	A	38	750	1.44	0.0341	
D4	Hirama et al. (1995)	100	FCC	A	54	810	4.47	0.0743	
D5	Horio et al. (1992)	50	FCC	A	60	1,000	7.57	0.106	
			Sand	B	106	2,600	108.5	0.647	
D6	Chang and Louge (1992)	200	Plastic	B	234	1,440	135.7	1.508	
			Steel	B	67	7,400	127.1	0.807	
D7	Bai et al. (1998)	76	FCC	A	70	1,600	19.23	0.210	
D8	Li et al. (1988)	90	FCC	A	54	929	5.13	0.0853	The choking for D8 to D10 refers to the regime transition between dilute suspension and fast fluidization.
D9	Takeuchi et al. (1986)	100	FCC	A	57	940	6.10	0.0914	
D10	Yang and Sun (1990)	30	Gel-I	A	165	794	124.9	0.463	
			Gel-II	B	325	794	954.3	1.109	
			Mo-Cat	A	85	1,487	32.0	0.273	
D11	Bai and Kato (1995)	66, 97, 150	FCC	A	76	1,623	15.62	0.187	See §
D12	Drahoš et al. (1988)	55	Phos.-I	B	120	2,550	154.4	0.748	See ‖
			Phos.-II	B	200	2,550	715.0	1.446	
D13	Satija et al. (1985)	107	Sand-I	B	155	2,446	319.2	1.008	See note #
			FCC	A	65	2,605	25.07	0.287	
			(b) *Classical choking*						
D14	Zenz (1949)	45	Salt	B	167	2,100	342.8	0.988	The choking of D14 to D18 are all defined as the onset (appearance) of plugs or slugs.
			GBs	B	588	2,483	17,692	4.308	
D15	Lewis et al. (1949)	32	GBs-I	A	40	2,483	5.6	0.12	
			GBs-II	B	100	2,483	87.0	0.572	
			GBs-III	B	280	2,483	1,910.4	2.187	
D16	Ormiston (1966)	25	Sand-I	B	120	2,659	161.0	0.772	
			Sand-II	B	151	2,659	320.9	1.039	
			Sand-III	B	225	2,659	1,061.6	1.738	
			Sand-IV	B	265	2,659	1,734.4	2.147	
D17	Mok et al. (1989)	20	Sand	B	210	2,620	850.4	1.572	
D18	Bai et al. (1998)	76	FCC	A	70	1,600	19.2	0.21	

*Air, with $\rho_f = 1.184$ kg/m^3 and $\mu = 1.82\times10^{-5}$ kg/(m·s), was used by all the measurements except for Chang and Loung (1992) who employed $\rho_f = 0.3$ kg/m^3 and $\mu = 2.0\times10^{-5}$ kg/(m·s) for plastic, and $\rho_f = 1.49$ kg/m^3 and $\mu = 1.6\times10^{-5}$ kg/(m·s) for steel.
†The type of particles was classified in accordance with Geldart (1973).
‡The differential pressure drops were measured both above and below the solid feed entrance on the riser, of which the ones above the entrance were used for the determination of choking.
§The onset of a constant voidage (differential pressure drop) in the measuring section after the dilute suspension flow collapses into a denser condition.
‖The maximal differential pressure drop measured above the lower dense bed section when reducing gas velocity successively from dilute suspension operation.
#Stepwise change in dominant frequency or standard deviation of differential pressure drop or in the differential pressure drop (voidage) itself measured at the dilute suspension collapse.

tion, this pressure drop is also related to the measurement methods. First, it is seriously affected by the measuring position. At a lower bed level, the effect of solid acceleration causes a larger pressure drop (Arena et al., 1985; Weinstein and Li, 1989). This can be corroborated by the measurements at different values of H_d given by Yerushalmi and Cankurt (1979) for particle HFZ-20 and in the present study for solid FCC-I (in the riser of $D_t = 97$ mm). Second, the length of the measuring section also has a significant effect on the acquired values. As a result of the gradual accumulation of particles in the bottom region of the column, a shorter measuring interval should give rise to a larger differential pressure drop averaged over the measuring section. Therefore, Xu et al. (1999a) stated that it is currently difficult to identify a unique $\Delta P_{d,\mathrm{ck}}/\Delta Z$ dominating the dilute suspension collapse.

Figure 3b shows the apparent solid concentrations $1-\epsilon_{\mathrm{ck,app}}$ calculated from the critical differential pressure drops plotted in Figure 3a. It is clear that as the particle becomes heavier and larger, which corresponds to an increased Archimedes number (see Ar in Table 3), the collapse of the dilute suspension occurs at a smaller apparent solid concentration. This smaller $1-\epsilon_{\mathrm{ck,app}}$ actually shows that the dilute suspension flow more easily collapses into dense flows in the case of heavier and larger particles, a general result regarding the fluidization characteristics of different particles. Nonetheless, Figure 3a shows that $\Delta P_{d,\mathrm{ck}}/\Delta Z$ fails to adhere to such a relationship. This is because the effect of solid density ρ_p is included in the values of $\Delta P_{d,\mathrm{ck}}/\Delta Z$. Essentially, $1-\epsilon_{\mathrm{ck,app}}$ consists of three components, the actual solid concentration, solid acceleration, and solid-to-wall friction. Van

Swaaij et al. (1970) demonstrated that the shear friction on the riser wall is less than 10% of the measured pressure drop, even in very dense conditions. On the other hand, the measurements using both pressure taps and a direct solid trap by Arena et al. (1985) showed that the contribution of acceleration is closely related to the solid concentration itself. At a given bed elevation, the higher the solid concentration is, the larger is the acceleration proportion in the apparent value. Without losing the generality, it can thus be suggested that the same $\Delta P_{d,\mathrm{ck}}/\Delta Z$ and $1-\epsilon_{\mathrm{ck,app}}$ show essentially the equality in actual solid concentration. By measuring the total solid amount fed to a riser, Bai et al. (1998) found that the solid holdup in the riser at the accumulative choking was independent of gas velocity. This shows the same flow physics as that demonstrated in Figures 3 and 4.

Quantification

Parametric dependence

In addition to the measurements carried out in this study, the major experimental data available in the literature were also compiled to develop a unified correlation for the saturation carrying capacity or for the gas velocity of the accumulative choking. Table 3 summarizes the experimental conditions of all the compiled data, together with their determination methodology listed under "choking definition." The particle diameters in the table usually refer to the surface-to-volume mean values, and the particle terminal velocities were calculated with respect to such average particle sizes by using the drag coefficient equation of Xu and Li (1998). While the data sets D1 to D5 were derived using the same method as that illustrated in Figure 2 from differential pressure drop diagrams, the sets D6 and D7 are based on the onset of the rapidly increased solid concentration observed at the dilute suspension collapse. The data from D8 to D10 are obtained by reading the regime demarcation loci between dilute suspension and fast fluidization. Although somewhat different determination approaches have been employed by the authors of sets D11 to D12, their definitions imply actually the same flow physics as those of D1 to D10. The saturation carrying capacity of Bai and Kato (1995) refer to the solid circulation rate at the onset of a little changed cross-sectional average voidage (differential pressure drop) in the measuring section. This suffers a time lag in comparison with the collapsing point determined at the start of the particle accumulation within the measuring section, but it usually leads to little deviation for the measurement of the saturation carrying capacity. According to Figure 2, the solid flow rate varies little between the dilute suspension collapse and the onset of the constant solid concentration. When gas velocity is gradually reduced (solid inventory being specified), a maximal differential pressure drop has been detected by Drahoš et al. (1988) above the bottom dense bed and was considered to be the choking point. It was explained that this maximal differential pressure just corresponds to the start of the particle accumulation at the riser bottom. The stepwise changes in differential pressure drop and its dominant frequency defined by Satija et al. (1985) essentially denote the hydrodynamic phenomena of the dilute suspension collapse; accordingly, the choking they defined certainly belongs to the accumulative type.

For reference and for later comparisons with the calculations from various correlations, all the compiled G_s^* and their corresponding gas velocities U_{ck} will be summarized in Table A1 of the Appendix. As shown in Table 3 and Table A1, a total of 158 experimental data points have been obtained and they have a wide range of measurement conditions with particles from group A to group B and riser diameters from 30 mm to 200 mm. The data from rather large units are expected, but there are few such reports in the literature (to our knowledge). While all the data are with respect to different gas velocities, only the present work (set D1) considers the influences of unit diameter upon the saturation carrying capacity. In theory, the transition of the longitudinal voidage profiles from uniform to nonuniform can also be utilized to determine G_s^* and U_{ck} (Xu et al., 1999b). Such data were excluded in this article, since most voidage profiles, such as those from Li and Kwauk (1980), Li et al. (1981), and Bai et al. (1992), are not detailed enough to precisely read the choking point.

Figure 5 shows the saturation carrying capacities for particles FCC-I (5a), silica sand (5b) and alumina (5c) measured in this work. In all cases, the solid circulation rate G_s^* increases with increasing gas (choking) velocity U_{ck}. Nevertheless, a different variation of G_s^* with D_t is manifested in Figure 5a in comparison with that in Figures 5b and 5c. With increasing the riser (column) diameter, the saturation carrying capacity increases for FCC-I, but decreases for silica sand and alumina. This reverse dependence of G_s^* upon D_t for groups A and B particles was interpreted by Xu et al. (1999b, 2000) in terms of the different influences for different particles of the riser diameter upon the bed density (the bed density referring to either the solid holdup in the whole riser or the solid concentration at a given bed position). As D_t increases, the bed density was also found to increase for light and small particles (FCC-I), but to increase for heavy and large particles (silica sand). In addition, Figures 5b and 5c indicate that the difference in G_s^* due to the influence of the riser diameter appears larger for silica sand (group B particles). Therefore, not only does the riser diameter have pronounced influence on the saturation carrying capacity, but the influence is also closely related to the properties of particles.

Correlation development

Based on Figure 5, one can postulate that G_s^* should be subject to the following formulation

$$\frac{G_s^*}{\rho_p u_t} = \mathrm{Fun}\left(Ar, \frac{U_{\mathrm{ck}}-u_t}{u_t}, \frac{D_t}{d_p}\right), \tag{1}$$

where Ar is used to rend the material properties (of both solids and fluid) into a unique parameter. Figure 6 shows the dependence of $G_s^*/(\rho_p u_t)$ on the dimensionless gas velocity $(U_{\mathrm{ck}}-u_t)/u_t$, with 6a and 6b for the data of this study and 6c for a few other literature measurements. While all of the data manifest a linear relationship between the two parameters plotted, Figures 6a and 6b further demonstrate that the slope of the resultant straight line is a constant independent of riser diameter for a given kind of particles. Thus, we have

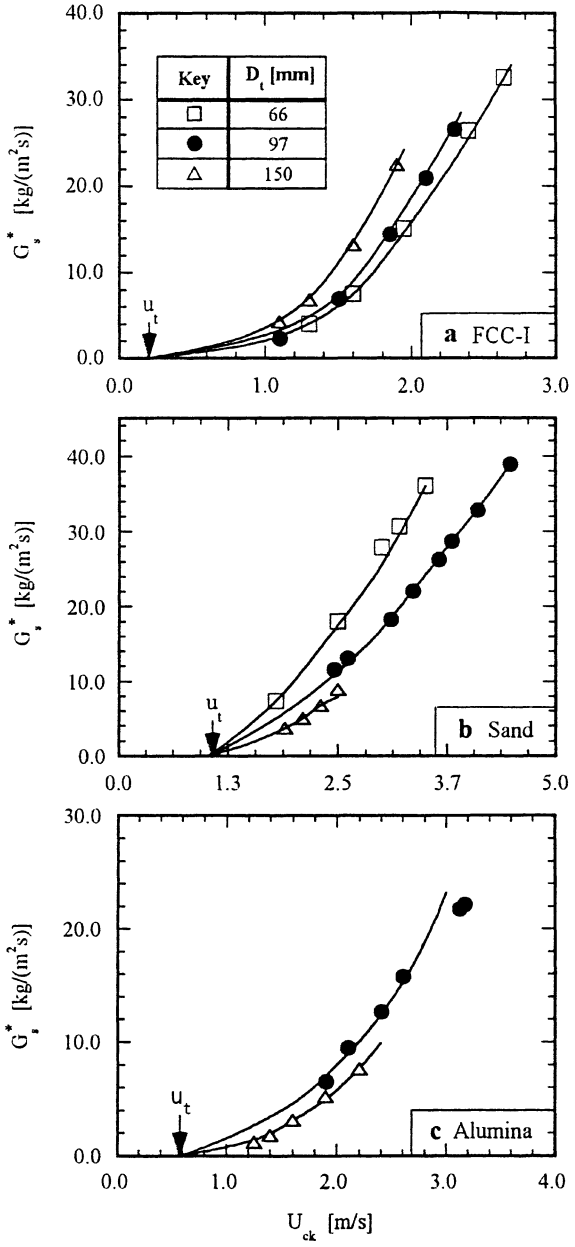

Figure 5. Saturation carrying capacity with respect to gas velocity for different particles in different risers.

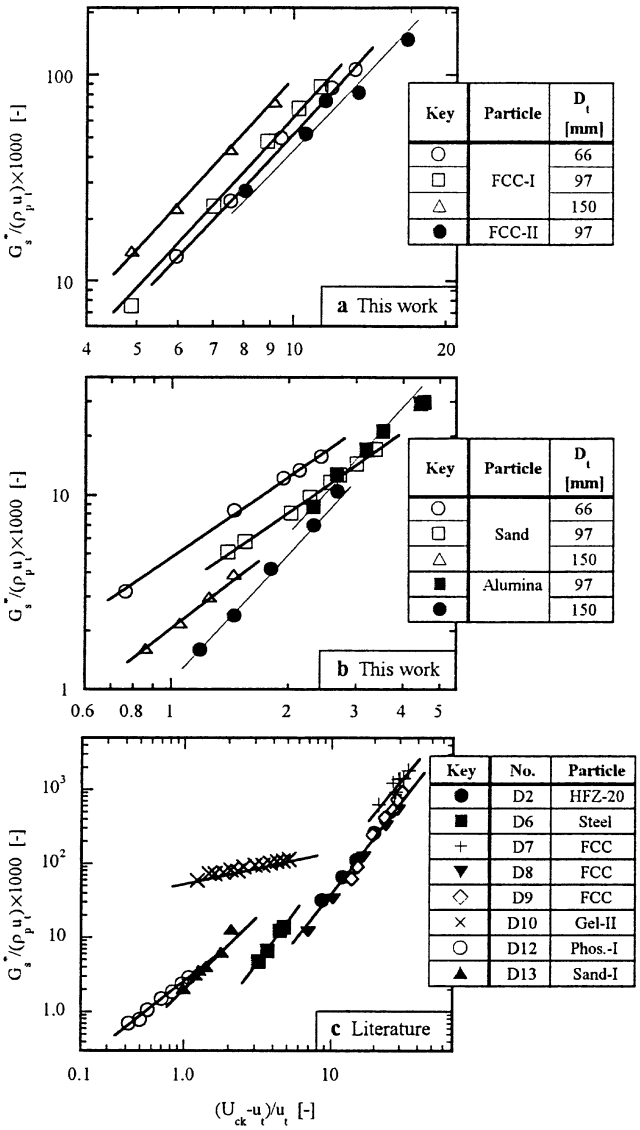

Figure 6. Correlation of the saturation carrying capacity with gas velocity for the measurements both by this work (a and b) and in the literature (c).

$$\frac{G_s^*}{\rho_p u_t} \propto \left(\frac{U_{\mathrm{ck}} - u_t}{u_t}\right)^a, \tag{2}$$

where the index a is related to the material properties (with only the solid properties examined here). By determining the parameter a from Figure 6 for all the compiled data indexed in Table 3, we finally obtain the correlation of a with the Archimedes number, Ar, as shown in Figure 7. Although the data are rather scattered, due to the wide sources of G_s^* and U_{ck}, the factor a generally decreases with increases in Ar. By using a linear relationship to average the correlation in Figure 7, we can have an equation as follows

$$a = 2.355 - 0.00191\,Ar. \tag{3}$$

With Eqs. 2 and 3, the influence of the column diameter D_t on G_s^* can then be expressed with an intermediate parameter defined by

$$\mathrm{Fun}(D_t) = \left(\frac{G_s^*}{\rho_p u_t}\right)\left(\frac{U_{\mathrm{ck}} - u_t}{u_t}\right)^{-a}. \tag{4}$$

This parameter is plotted in Figure 8 and computed from the experimental G_s^* for particles FCC-I, alumina and silica sand measured in this study. In fact, at the moment there are not any other data available for the production of this relationship (referring to Table 3). The figure evidently shows that for given particles, the saturation carrying capacities for different gas velocities but the same column diameter have

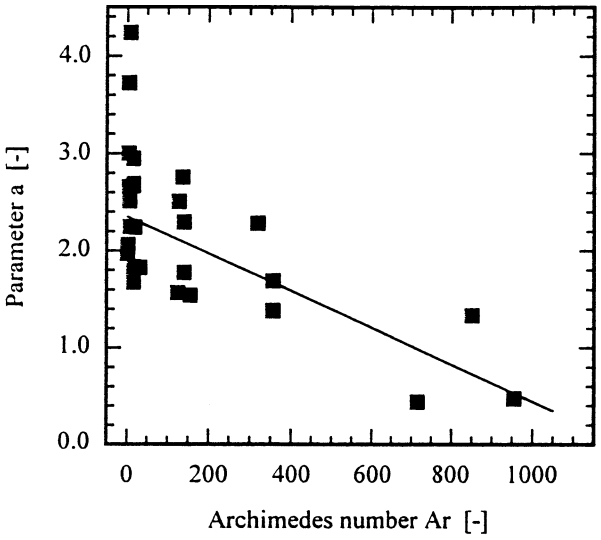

Figure 7. Correlation of parameter *a* calculated from the compiled experimental saturation carrying capacity with the Archimedes number *Ar*.

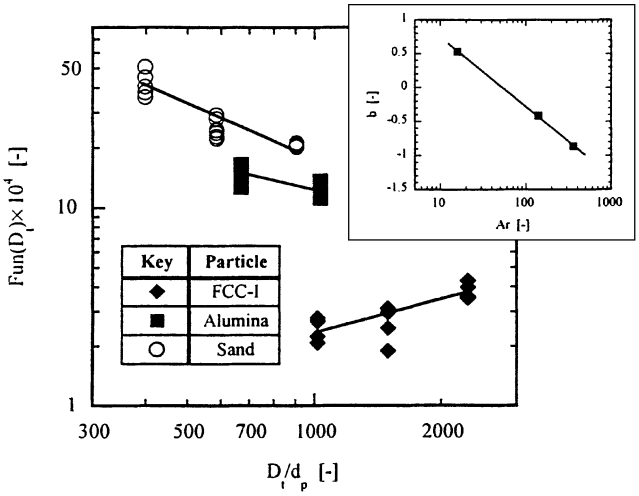

Figure 8. Dependence of the saturation carrying capacity on column diameter for different particles (the side figure correlating parameter *b* with the Archimedes number *Ar*).

identical values of Fun(D_t). Moreover, Fun(D_t) linearly varies with the dimensionless column diameter D_t/d_p for every species of particles, thus leading to

$$Fun(D_t) \propto \left(\frac{D_t}{d_p}\right)^b, \tag{5}$$

where the factor b represents the slope of the correlated line. Corresponding to Figure 5, b should be positive for FCC-I but negative for alumina and silica sand. However, the negative value for alumina is smaller than that for silica sand, implying that the riser diameter affects G_s^* to a less degree in the case of alumina. The side figure in Figure 8 correlates b with Ar, revealing again a linear relationship, and, therefore, we have

$$b = 1.740 - 0.441 \ln Ar. \tag{6}$$

As a result of Eqs. 2, 4 and 5, Eq. 1 can then be extended to

$$\frac{G_s^*}{\rho_p u_t} = K\left(\frac{U_{ck} - u_t}{u_t}\right)^a \left(\frac{D_t}{d_p}\right)^b. \tag{7}$$

On the basis of all the compiled experimental data, the parameter K is finally formulated as

$$K = \begin{cases} 0.0158\left(\dfrac{Ar}{100}\right)^{4.093}, & Ar \le 50 \\ 0.00923\left(\dfrac{Ar}{100}\right)^{3.344}, & Ar \ge 50 \end{cases} \tag{8}$$

Thus, the estimation of the saturation carrying capacity G_s^* from a given gas velocity U_{ck} or of the choking velocity U_{ck} from a prescribed solid flow rate G_s^* can be done using Eqs. 7, 3, 6 and 8 for a system having specified facility size (D_t) and material properties (Ar).

Accuracy evaluation

With the intention of not only validating the correlation developed above, but also sequencing the accuracy of the correlations available in the literature, Figure 9 compares the saturation carrying capacities of the complied experimental data and the values calculated from all the 14 correlations summarized in Table 1. The data listed in Table A1 of the Appendix are all used for this comparison (158 points in total). Although correlations C5 and C10 were originally proposed for polydisperse particles, they are similarly cited here by considering that a mean diameter can be used to represent the sizes of multisized particles. As shown in Figure 9, the graphical comparison is made in two different scales, with the main sets in a smaller scale of 0 ~ 120 and the side sets in a full scale of 0 ~ 600 that can cover the whole range of the data. In addition, the correlations C5 and C6, as well as C8 and C9, are plotted in the same figure, since we noted that both the correlations actually have very similar predictions.

As can be seen in Figure 9, the computed values from C2 and C5 to C9 greatly deviate from the experimental measurements, showing their inapplicability to the prediction of the accumulating choking and dilute suspension collapse. Among the remaining correlations, the side figures indicate that C11 from Bi and Fan (1991) and C13 from Xu et al. (1999b) have good accuracy in the whole range of G_s^*, while the correlation C14 developed in this work has the next best accuracy. However, this is a result misled by the wide plotting range of the site figure since the main set figure demonstrates that the calculations from both C11 and C13 are more diversified than that from C14. As a matter of fact, $G_{s,cal}^*$ from C11 is usually

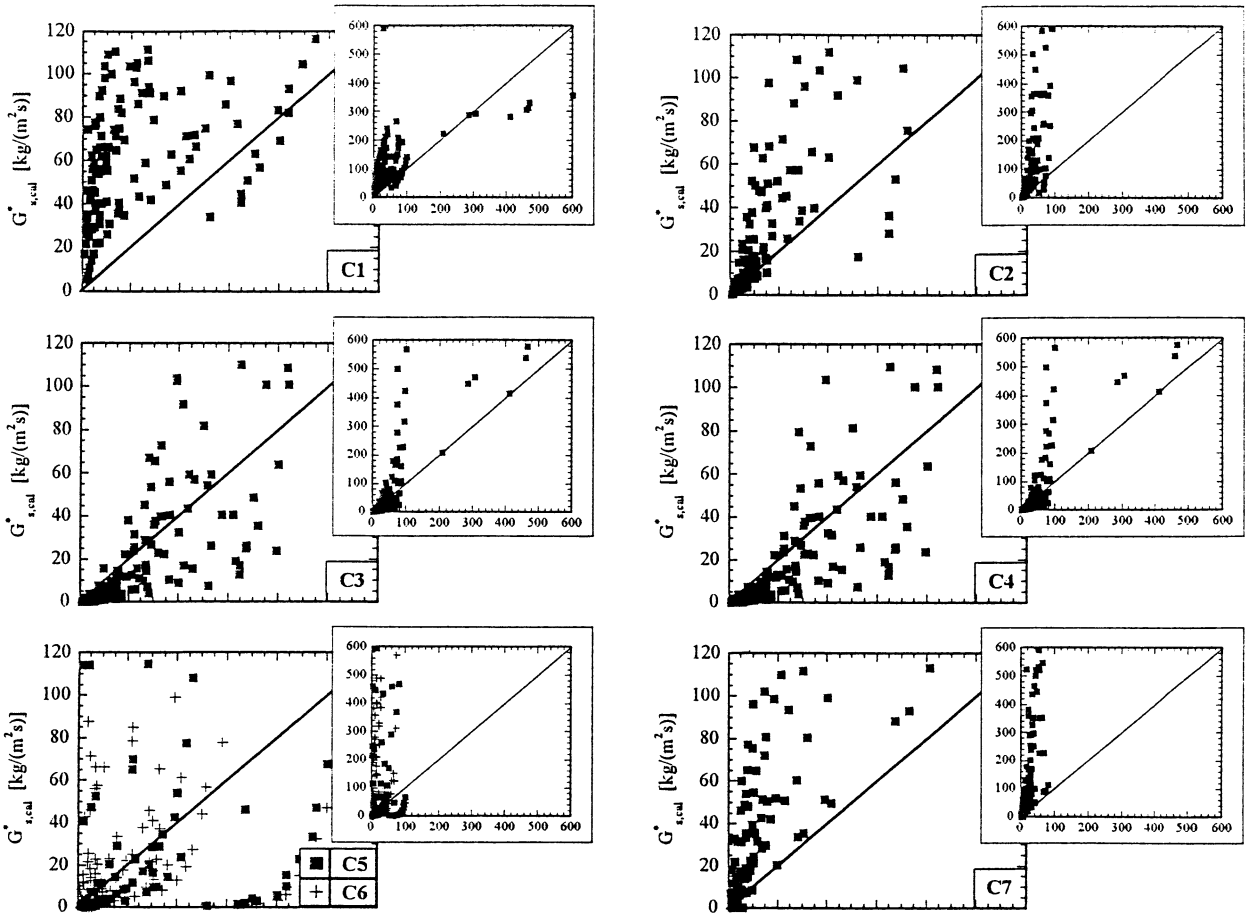

Figure 9. Saturation carrying capacity: experiments vs. calculations from various correlations for accumulative choking (continued).

somewhat lower than $G^*_{s,\exp}$ in the range of $G^*_s = 0 \sim 120$ kg/(m$^2\cdot$s). On the other hand, of the compiled G^*_s listed in Table A1, only the data of D7 from Bai et al. (1998) are in the range of $120 \sim 600$ kg/(m$^2\cdot$s), while all the others are less than 120 kg/(m$^2\cdot$s). Therefore, more experimental measurements are needed to acquire a more reliable validation of the correlation accuracy in the high solid flow rate region of $G^*_s = 120 \sim 600$ kg/(m$^2\cdot$s). Of the correlations C1, C3, C4, C10 and C12, those showing the greatest deviations are C3 and C4, while C10 and C12 manifest relatively good accuracy. Although the predictions from C3 and C4 appear around the experimental data in the main set figure, the corresponding side figure shows that the calculated solid flow rates are much larger than the measured ones in many cases. The correlation C1 usually gives much higher calculated values than experimental measurements in $G^*_s = 0 \sim 120$ kg/(m$^2\cdot$s).

A more detailed comparison of experiments and calculations for correlations C1, C3, C4, and C10 to C14 can be implemented by analyzing the values of $G^*_{s,\exp}$ and $G^*_{s,\mathrm{cal}}$ listed in Table A1 in the Appendix. A ratio $\Re = G^*_{s,\mathrm{cal}}/G^*_{s,\exp}$ is defined to quantitatively show the accuracy of the calculation. Thus, a highly accurate correlation should have an $\Re$ around 1.0. For all the correlations shown in Table A1, the $\Re$ corresponding to each $G^*_{s,\exp}$ can be calculated from its $G^*_{s,\mathrm{cal}}$. By treating the total 158 values of $\Re$ for each correlation as a data sample, the following parameters can be obtained by statistical analysis

$$\text{Average: } \Re_{\mathrm{av}} = \sum \Re_i/158, \quad \text{Maximum: } \Re_{\max} = \mathrm{Max}(\Re_i),$$
$$\text{Minimum: } \Re_{\min} = \mathrm{Min}(\Re_i), \quad i = 1, \ldots, 158. \tag{9}$$

Noting that both $\Re_{\max}$ and $\Re_{\min}$ could be seriously affected by one or two data points that are inaccurately measured, the low and the upper limits of $\Re$ are calculated at a credit of 90%, that is

$$\text{Low limit: } \Re_{\mathrm{low}} = \Re_{F=5.0\%}, \quad \text{Upper limit: } \Re_{\mathrm{up}} = \Re_{F=95.0\%}, \tag{10}$$

where F denotes the accumulative distribution function with $F = 0$ at $\Re = \Re_{\min}$ and $F = 100\%$ at $\Re = \Re_{\max}$.

Shown in Table 4 are the parameters defined above for the correlations listed in Table A1. In most cases, such as for C1, C3, C4, C10 and C13, a large difference prevails between $\Re_{\max}$ and $\Re_{\mathrm{up}}$, as well as between $\Re_{\min}$ and $\Re_{\mathrm{low}}$. On the other hand, there are only 8 data points between $F = 5\%$ and above $F = 95\%$ for the data sample with a total number of data points of 158. This obviously implies that the use of

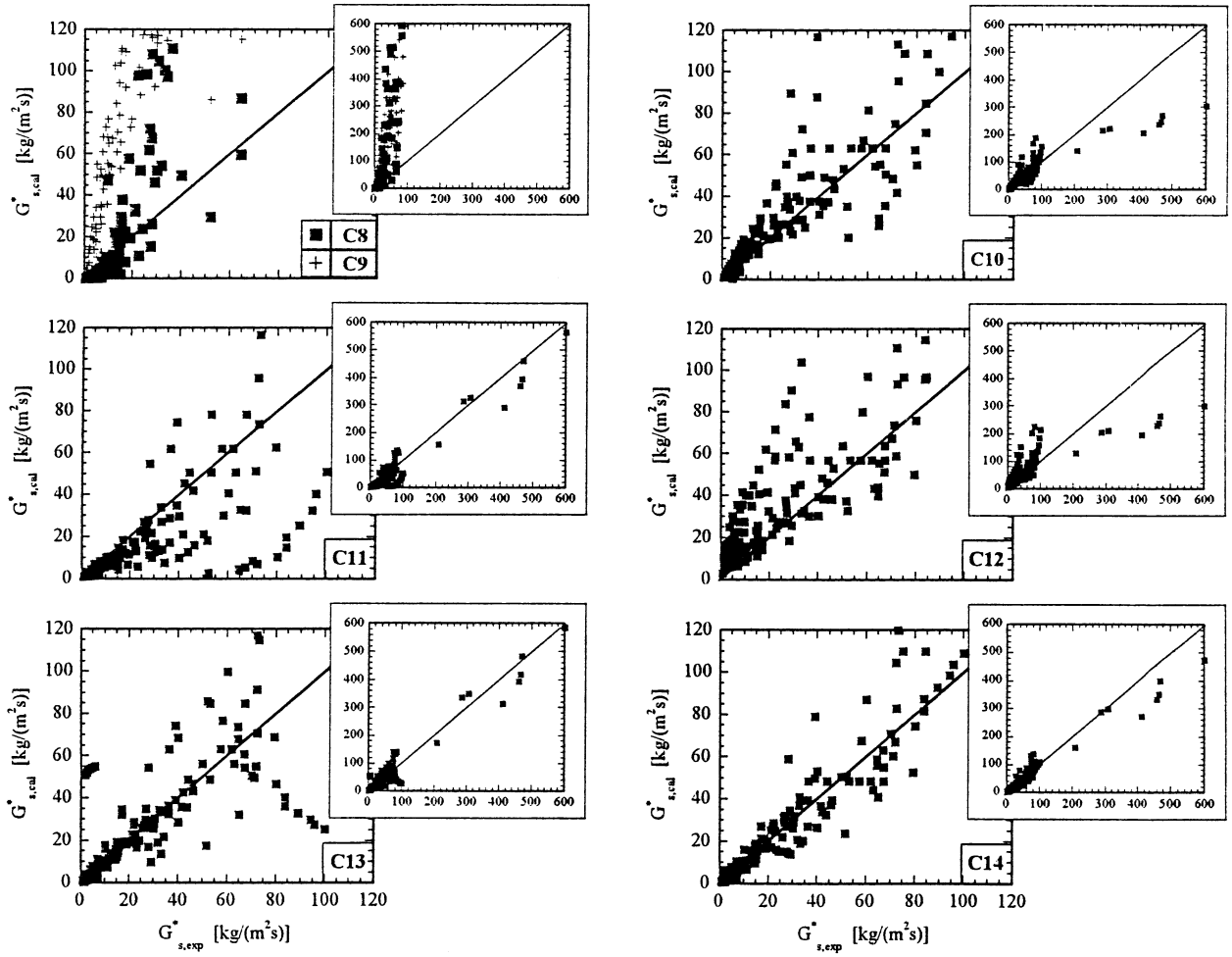

Figure 9. (Continued) Saturation carrying capacity: experiments vs. calculations from various correlations for accumulative choking.

$\Re_{up}$ and $\Re_{low}$, instead of $\Re_{max}$ and $\Re_{min}$, would be more reliable for evaluating the error range of the predictions from a correlation. An accurate correlation should possess not only a $\Re_{av}$ near unity, but also small deviations of $\Re_{up}$ and $\Re_{low}$ from $\Re_{av}$. Based on these criteria, Table 4 then shows that the most accurate correlation is C14, and the next most accurate one is C11. The $\Re_{av}$ equating 0.729 of C11 also means that the computed values from this correlation are usually smaller than the experimental measurements. Among the other correlations compared in Table 4, C13 and C10 can create acceptable predictions in most cases. Nevertheless, minus solid flow rates are probable for C10 ($\Re_{min} = -4.007 < 0$), while much higher predictions than experimental measurements seem possible for C13 ($\Re_{max} = 25.160 \gg 1.0$). The correlation C12 usually predicts G_s^* with relatively good accuracy ($\Re_{av} = 2.251$), whereas C3 and C4 can be considered to be very poor for this prediction (seeing also Figure 9).

In conclusion, the five most-accurate correlations of all the 14 correlations compared in Figure 9 and in Table 4 can be sequenced, on average, as follows

$$\text{C14} \geq \text{C11} \geq \text{C13} \geq \text{C10} \geq \text{C12} \qquad (11)$$

However, C13 and C10 should be carefully used since they may produce unreasonable results in some rare cases, that is, either negative solid flow rates or greatly deviated values.

Table 4. Accuracy Identification with Statistical Parameters for Accumulative Choking

Correlation No.	C1	C3	C4	C10	C11	C12	C13	C14
Average, $\Re_{av}$	6.219	0.966	0.931	1.090	0.729	2.251	1.623	1.056
Maximum, $\Re_{max}$	34.094	6.964	6.934	3.211	1.959	8.734	25.160	2.107
Minimum, $\Re_{min}$	0.593	0.0	0.001	−4.007	0.055	0.474	0.254	0.312
Upper limit, $\Re_{up}$	17.414	2.672	3.040	2.205	1.335	5.720	1.901	1.679
Low limit, $\Re_{low}$	0.761	0.113	0.116	−0.847	0.224	0.629	0.412	0.574

Discussion

On the preceding results

It was demonstrated in MECHNISM that the dilute suspension collapse and accumulative choking are dominated by an identical differential pressure drop, and, essentially, the same solid concentration, over the measuring section. This allows the voidage at choking ϵ_{ck} to be accurately predicted and enables the choking to be fundamentally formulated. Nonetheless, implementation of this objective requires more work based on more unified experimental methods. With this recognition, a new correlation, as shown in Eq. 7, was developed in this work, although it is not directly related to the observed choking mechanism. In a long period, the empirical correlation is perhaps the only effective tool available for the choking prediction.

The newly developed correlation C14 shows the best accuracy for predicting G_s^* or the accumulative choking velocity U_{ck}. This notwithstanding, two points regarding this correlation are noteworthy: the dependence of G_s^* on the column diameter D_t (factor b) and the application range of the correlation. Because Eq. 6 for the parameter b is merely based on the measurements obtained in this study, more work is needed to improve this equation. It is particularly important to experimentally find a flow system that is little affected by the column diameter D_t, namely, a system characterized by $b = 0$. The data used for the accuracy validation are in $30 \le D_t \le 200$ mm and $Ar < 1{,}000$; thus, the correlation is definitely applicable to this range. It might also be extended to units with rather larger (> 200 mm) or smaller (< 30 mm) D_t, but further validation using experimental data derived from those rigs would be necessary. Again, Eq. 3 demonstrations that the values of parameter a become minus when $Ar > 1{,}233$, which actually implies that the correlation is applicable only to systems with $Ar < 1{,}233$ (based on the concept that G_s^* increases with increasing U_g). In general, this range should cover most practical gas-solid systems of particles from group A to group B. On the other hand, Eq. 3 also implies that the effect of gas velocity upon the saturation carrying capacity decreases as Ar increases. It is thus considered that the reversion of the factor a from positive to negative at a particular Ar possibly implicates with some peculiar flow physics, although nothing is known at present.

As mentioned by Eq. 11, correlation C11 was finally concluded as an accurate equation for the accumulative choking, consisting with the result of Bi et al. (1993). However, the correlations of Yang (1975, 1983), that is, C3 and C7, were shown to have serious deviations in Figure 9, whereas they have been suggested to be reliable for choking prediction by Briens and Bergougnou (1986) and Bi et al. (1993). This difference is thought to be due not only to the limited data employed by other researchers, but also to the different methods used for the accuracy evaluation. The average relative error (deviation), a parameter similar to $\mathcal{R}_{av}$, has been widely utilized as the evaluation criterion by literature comparisons. Here, it is considered that the use of the statistical data, particularly $\mathcal{R}_{av}$ only, is insufficient for the judgment. In fact, Table 4 shows also that the accuracy of C3 and C4 should not be very poor since the values of their $\mathcal{R}_{av}$ ($0.93 \sim 0.7$) are near unity, while their $\mathcal{R}_{up}$ ($2.0 \sim 3.0$) and $\mathcal{R}_{low}$ ($0.11 \sim 0.12$) are not much different from 1.0. In addition, the calculation of the particle terminal velocity u_t may also affect the accuracy evaluation because most correlations have had u_t correlated. Here, the drag coefficient equation (for a single particle) proposed by Xu and Li (1998) was used for the calculation of u_t.

Prediction of classical choking

Even for particles of groups A and B, calculation of the classical choking (type C choking) is also sometimes needed. Therefore, some well-documented experimental data of classical choking were compiled to examine the ability of all 14 correlations for predicting this type of choking. The experimental conditions are summarized in Table 3, and the data, 52 points in total, will be listed in Table A2 in the Appendix. Here, only the data for particles of groups A and B are selected, considering that most solids used in vertical conveying systems, especially in CFBs, belong to these two groups. In fact, separate evaluation for each different group of particles is necessary, as was done by Chong and Leung (1986).

The comparison of experiments and calculations is graphically presented in Figure 10. Considering that all of the data in Figure 9 have Archimedes numbers Ar less than 1,000, Figure 10 distinguished the data for $Ar < 1{,}000$ from those for $Ar > 1{,}000$ by using different legends. However, C13 and C14 were applied only to the case of $Ar < 1{,}000$, due to the limitation of their formulations for parameter a. Comparing to Figure 9, one can see that those correlations that predicted the accumulative choking with relatively good accuracy, such as C10 to C14, exhibit poor accuracy here for the classical choking (usually underestimating). In contrast, the other correlations that overestimated the type A choking, such as C2, C7 to C9, manifest good accuracy in predicting the type C choking. This consists with the result of theoretical analysis that, at a given gas velocity, the accumulative choking corresponds to a lower solid flow rate (G_s^*), or, in turn, for a specified solid flow rate, the type C choking occurs at a lower gas velocity. The result clarifies again that it is impossible to use one correlation for both type A and type C choking, as stressed by Bi et al. (1993). In addition, Figure 10 clearly demonstrates that most correlations underestimate the critical solid flow rates G_s^c for systems with higher Archimedes numbers, such as, $Ar > 1{,}000$ in the figure, evidencing the necessity of distinguishing the experimental data with different Ar.

In order to rank the accuracy of the correlations for predicting the type C choking, the calculated critical solid flow rates from the best six correlations obtained from Figure 10 are further compared in Table A2 in the Appendix. Their statistical data, that is, $\mathcal{R}_{av}$, $\mathcal{R}_{max}$, $\mathcal{R}_{min}$, $\mathcal{R}_{up}$, and $\mathcal{R}_{low}$, are summarized in Table 5. Based on both Figure 10 and Table 5, it can be seen that the most accurate correlation is C2 proposed by Yousfi and Gau (1974). It has not only a $\mathcal{R}_{av}$ close to 1.0, but also such $\mathcal{R}_{max}$ ($\mathcal{R}_{up}$) and $\mathcal{R}_{min}$ ($\mathcal{R}_{low}$) that have the smallest deviations from $\mathcal{R}_{av}$. The accuracy of C8 is also acceptable, but the values of its $\mathcal{R}_{av}$ (0.865), $\mathcal{R}_{max}$ ($\mathcal{R}_{up}$) and $\mathcal{R}_{min}$ ($\mathcal{R}_{low}$) greatly deviate from unity. Although C9 has a $\mathcal{R}_{av}$ (0.946) that appears closest to 1.0, Figure 9 shows that the correlation fails to unify the predictions for systems with different Archimedes numbers. The correlation C7 seems to be good for the case of $Ar < 1{,}000$, but poorly predicts the systems of $Ar > 1{,}000$. Nonetheless, C1 and C7 are definitely more accurate than C12, and therefore the six correlations

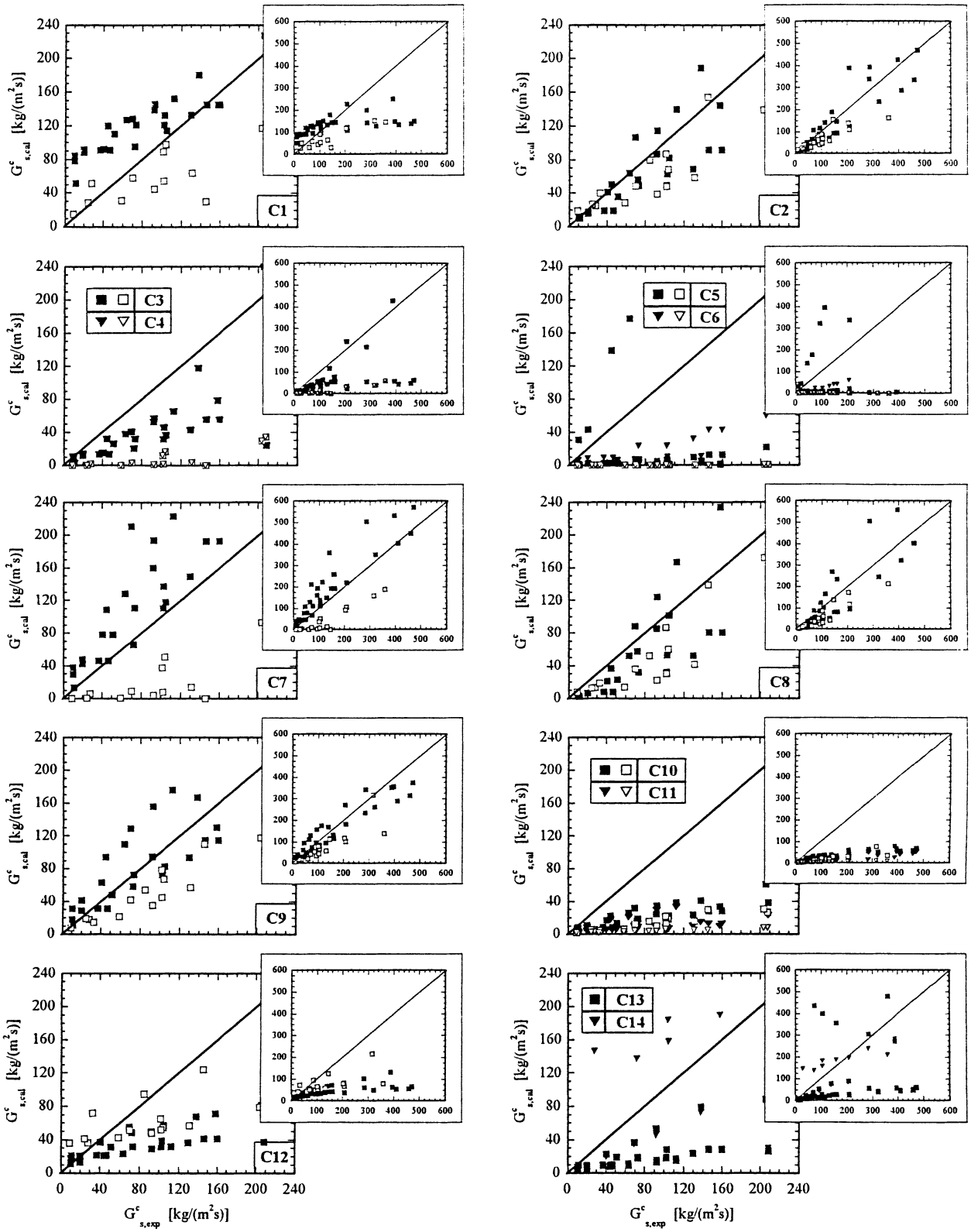

Figure 10. Critical solid flow rate: experiments vs. calculations from various correlations for classical choking (solid marks: *Ar* < 1,000, open marks: *Ar* > 1,000).

Table 5. Accuracy Identification with Statistical Parameters for Classical Choking

Correlation No.	C1	C2	C7	C8	C9	C12
Average, $\Re_{av}$	1.341	0.905	1.244	0.865	0.946	0.619
Maximum, $\Re_{max}$	8.562	2.121	3.838	4.986	3.195	4.002
Minimum, $\Re_{min}$	−1.817	0.424	−0.415	0.172	0.372	0.123
Upper limit, $\Re_{up}$	4.627	1.771	3.283	3.026	1.990	1.885
Low limit, $\Re_{low}$	0.261	0.448	0.006	0.238	0.414	0.147

have the following accuracy sequence

$$C2 \geq C8 \geq C9 \geq C7 \geq C1 \geq C12 \tag{12}$$

For particles belonging to groups A and B, the correlation C2 has also been tested as the most accurate equation by Chong and Leung (1986) and Bi et al. (1993). Biswas and Leung (1987) found that this correlation actually underestimated the regime demarcation gas velocities between fast fluidization and lean-phase conveying. With Eqs. 11 and 12, this result definitely becomes certain because such a transition denotes the type A choking, and C2 is accurate only for type C choking that occurs at a lower gas velocity for a given solid flow rate.

Nonetheless, it is worthwhile to note that the correlation C2 does not take the column diameter D_t into account, while the data used for the accuracy test, as shown in Tables 3 and A1, have a limited range of D_t in 20 ~ 80 mm. Equation C8 from Mink (1983) has lower accuracy than C2 does, but it should still be recommended for its inclusion of D_t in the formulation. At the same time, one may be reminded that C8 has been identified as an inaccurate formulation for choking by Briens and Bergougnou (1986). This must be a result misled by the use of such experimental data without distinguishing particle groups. For type C choking of group D particles (monodispersed sizes), Chong and Leung (1986) have shown that the correlation C7 from Yang (1983), other than C2, had the highest accuracy (no estimation being made here for group D particles).

Conclusions

Experimental observations identified that the dilute suspension collapse, namely, the accumulative choking defined by Bi et al. (1993), of concurrent vertical conveying systems is dominated by an identical differential pressure drop over the measuring section that is usually at the bottom of the conveying column. This critical differential pressure drop is independent of the column diameter and gas velocity, but varies with the solid properties (diameter and density). It was also shown that the value of this critical differential pressure drop is seriously affected by the experimental method, such as the elevation and length of the measuring section.

The solid circulation rate at the dilute suspension collapse (accumulative choking), that is, the saturation carrying capacity, is closely related to the column diameter and particle properties. With increase in the column diameter, it increases for lighter and smaller particles (group A of Geldart's classification), but decreases for heavier and larger particles (group B, even A-B). This study showed that the contrary dependence of the saturation carrying capacity on the column diameter is bridged by a gradual transition from group A to group B particles.

Based on experimental observations, a predictive correlation was developed for the saturation carrying capacity. A total of 158 experimental data points was compiled to validate its accuracy by a comparison with 13 other literature correlations. It was demonstrated that the newly proposed correlation is most accurate for the prediction of the accumulative choking, while that of Bi and Fan (1991) shows also acceptable accuracy. This result is definitely valid for the systems with column diameters in 30 ~ 200 mm and Archimedes numbers less than 1,000 (groups A and B particles), while it might also be extended to facilities with larger diameters.

Using 52 literature data points in total, an additional test was conducted to evaluate the accuracy of all the 14 correlations for predicting the classical choking of particles belonging to groups A and B. The correlation of Yousfi and Gau (1974) was found to have the highest accuracy, but the equation of Mink (1983) is also recommendable due to its similar accuracy and the inclusion of column diameter in the formulation. Nevertheless, it should be noted that the experimental rigs covered by this evaluation had diameters only between 20 and 80 mm.

Some further works relevant to this study were also suggested by a discussion.

Notation

a = factor (parameter)
Ar = Archimedes number, $d_p^3 \rho_f g(\rho_p - \rho_f)/\mu$
b = factor (intermediate parameter)
c = factor (intermediate parameter)
d_p = surface-to-volume mean diameter, m
d_{pi} = diameter for fractional component F_{pi}, m
D_t = column (riser) diameter, m
F = accumulative distribution function, %
F_{pi} = accumulative fraction for d_{pi}, wt. %
Fr = Froude number [-], $U_g/(gd_p)^{0.5}$
g = gravitational acceleration, m/s^2
G_s = solids circulation (flow) rate, kg/(m^2·s)
G_s^* = saturation carrying capacity (for accumulative choking), kg/(m^2·s)
G_s^c = critical solid flow rate at classical choking, kg/(m^2·s)
H_d = elevation of measuring section (defined at its middle point), m
H_t = total height of conveying column (riser), m
K = parameter
ΔP_d = pressure drop measured over a bed section, kg/(m·s^2)
$\Delta P_{d,ck}$ = ΔP_d at dilute suspension collapse, kg/(m·s^2)
Re_t = Reynolds number, $\rho_f u_t d_p/\mu$
u_t = terminal velocity, m/s
U_{ck} = superficial gas velocity at choking, m/s
U_g = superficial gas velocity, m/s
Z = axial location, m
ΔZ = length of measuring section, m

Greek letters

ϵ_o = parameter related to choking
ϵ_{ck} = voidage at choking
$\epsilon_{ck,app}$ = apparent voidage at choking
μ = fluid viscosity, kg/(m·s)
ρ_p = particle density, kg/m^3
ρ_f = fluid density, kg/m^3
$\Re$ = ratio of calculated to experimental values

Subscripts

ck = at choking
cal = from calculation
exp = from experiment

Literature Cited

Arena, U., A. Cammarota, and L. Pistone, "High Velocity Fluidization Behavior of Solids in a Laboratory Scale Circulating Bed," *Circulating Fluidized Bed Technology I*, P. Basu, ed., Pergamon Press, Oxford, p. 19 (1985).

Bai, D., Y. Jin, Z. Yu, and J. Zhu, "The Axial Distribution of the Cross-Sectionally Averaged Voidage in Fast Fluidized Beds," *Powder Technol.*, **77**, 51 (1992).

Bai, D., and K. Kato, "Saturation Carrying Capacity of Gas and Flow Regimes in CFB," *J. Chem. Eng. Japan*, **28**, 179 (1995).

Bai, D., A. S. Issangya, and J. R. Grace, "A Novel Method for Determination of Choking Velocities," *Powder Technol.*, **97**, 59 (1998).

Bi, H. T., and L.-S. Fan, "Regime Transitions in Gas-Solid Circulating Fluidized Beds," *AIChE Meeting*, Los Angeles, Paper 101e (1991).

Bi, H. T., J. R. Grace, and J.-X. Zhu, "Types of Choking in Vertical Pneumatic Systems," *Int. J. Multiphase Flow*, **19**, 1077 (1993).

Biswas, J., and L. S. Leung, "Applicability of Choking Correlation for Fast-Fluid Bed Operation," *Powder Technol.*, **51**, 179 (1987).

Briens, C. L., and M. A. Bergougnou, "Simple Calculation Technique to Solve the Leung/Wiles Equation for the Choking Load of Multisize Particles in Pneumatic Transport Lines," *Can. J. Chem. Eng.*, **63**, 995 (1985).

Briens, C. L., and M. A. Bergougnou, "New Model to Calculate the Choking Velocity of Monosize and Multisize Solids in Vertical Pneumatic Transport Lines," *Can. J. Chem. Eng.*, **64**, 196 (1986).

Capes, C. E., and K. Nakamura, "Vertical Pneumatic Conveying: An Experimental Study with Particles in the Intermediate and Turbulent Flow Regimes," *Can. J. Chem. Eng.*, **51**, 31 (1973).

Chang, H., and M. Louge, "Fluid Dynamic Similarity of Circulating Fluidized Beds," *Powder Technol.*, **70**, 259 (1992).

Chong, Y. O., and L. S. Leung, "Comparison of Choking Velocity Correlations in Vertical Pneumatic Conveying," *Powder Technol.*, **47**, 43 (1986).

Day, J. Y., H. Littman, and M. H. Morgan III, "A New Choking Correlation for Vertical Pnematic Conveying," *Chem. Eng. Sci.*, **45**, 355 (1990).

Doig, I. D., and G. H. Roper, "The Minimum Gas Rate for Dilute-Phase Solids Transportation in a Gas Stream," *Aust. Chem. Eng.*, **1**, 9 (1963).

Drahoš, J. J. Čermák, R. Guardani, and K. Schügerl, "Characterization of Flow Regime Transition in a Circulating Fluidized Bed," *Powder Technol.*, **56**, 41 (1988).

Geldart, D., "Types of Gas Fluidization," *Powder Technol.*, **7**, 285 (1973).

Hariu, O. H., and M. C. Molstad, "Pressure Drop in Vertical Tubes in Transport of Solids by Gases," *Ind. Eng. Chem.*, **41**, 1148 (1949).

Hirama, T., H. Takeuchi, and T. Chiba, "Regime Classification of Macroscopic Gas-Solid Flow in a Circulating Fluidized Bed Riser," *Powder Technol.*, **70**, 215 (1992).

Hirama, T., K. Kuramoto, and T. Chiba, "Effects of Riser Height and Downcomer Solids Inventory on Dense-Bed Height in a Riser of CFB," *Fluidization VIII*, J. F. Large and C. Laguerie, eds., Engineering Foundation, New York, pp. 113–120 (1995).

Horio, M., H. Ishii, and M. Nishimuro, "On the Nature of Turbulent and Fast Fluidized Beds," *Powder Technol.*, **70**, 229 (1992).

Konrad, K., "Dense-Phase Pneumatic Conveying: A Review," *Powder Technol.*, **49**, 1 (1986).

Knowlton, T. M., and D. M. Bachovchin, "The Determination of Gas-Solids Pressure Drop and Choking Velocity as a Function of Gas Velocity in a Vertical Pneumatic Conveying Line," *Fluidization I*, D. L. Keairrns, ed., Hemisphere, Washington, DC, pp. 253–282 (1975).

Kwauk, M., and J. Li, "Fluidization Regimes," *Powder Technol.*, **87**, 193 (1996).

Leung, L. S., R. J. Wiles, and D. J. Nicklin, "Correlation for Predicting Choking Flowrates in Vertical Pneumatic Conveying," *Ind. Eng. Chem. Process Des. Dev.*, **10**, 183 (1971).

Leung, L. S., and R. J. Wiles, "A Quantitative Design Procedure for Vertical Pneumatic Conveying Systems," *Ind. Eng. Chem. Process Des. Dev.*, **15**, 552 (1976).

Leung, L. S., "Vertical Pneumatic Conveying: A Flow Regime Diagram and a Review of Choking Versus Non-Choking Systems," *Powder Technol.*, **25**, 185 (1980a).

Leung, L. S., "The Ups and Downs of Gas-Solid Flow—A Review," *Fluidization II*, J. R. Grace and J. M. Matsen, eds., Plenum Press, New York, p. 25 (1980b).

Lewis, W. K., E. R. Gilliland, and W. C. Bauer, "Characteristics of Fluidized Particles," *Ind. End. Chem.*, **41**, 1104 (1949).

Li, J., Y. Tung, and M. Kwauk, "Axial Voidage Profiles of Fast Fluidized Beds in Different Operating Regimes," *Circulating Fluidized Bed Technology II*, J. F. Large and P. Basu, eds., Pergamon Press, Oxford, pp. 193–205 (1988).

Li, J., M. Kwauk, and L. Reh, "Role of Energy Minimization in Gas/Solid Fluidization," *Fluidization VII*, O. E. Potter and D. J. Nicklin, eds., Engineering Foundation, New York, pp. 83–91 (1992).

Li, J., and M. Kwauk, *Particle-Fluid Two-Phase Flow*, *The Energy-Minimization Multi-Scale Method*, Metallurgy Industry Press, Beijing (1994).

Li, Y., and M. Kwauk, "The Dynamics of Fast Fluidization," *Fluidization III*, J. R. Grace and J. M. Matsen, eds., Plenum Press, New York, pp. 537–544 (1980).

Li, Y., B. Chen, F. Wang, Y. Wang, and M. Guo, "Rapid Fluidization," *Int. Chem. Eng.*, **21**, 670 (1981).

Matsen, J. M., "Mechanics of Choking and Entrainment," *Powder Technol.*, **32**, 21 (1982).

Matsumoto, S., and M. Marakawa, "Statistical Analysis of the Transition of the Flow Pattern in Vertical Pneumatic Conveying," *Int. J. Multiphase Flow*, **13**, 123 (1987).

Mink, W. H., "Critical Velocity in Solids Transport," *Particulate Systems: Technology and Fundamentals*, J. K. Beddow, ed., Hemisphere Publishing Corp., Washington, DC, p. 157 (1983).

Mok, S. L. K., Y. Molodtsof, J.-F. Large, and M. A. Bergougnou, "Characterization of Dilute and Dense Phase Vertical Upflow Gas-Solid Transport Based on Average Concentration and Velocity Data," *Can. J. Chem. Eng.*, **67**, 10 (1989).

Nomura, K., "Characterization of Dilute Suspension Collapse and Choking Phenomenon in Circulating Fluidized Bed Risers," Master Thesis (in Japanese), Gunma University, Kiryu, Japan (1998).

Ormiston, R. M., "Slug Flow in Fluidized Beds," Doctoral Thesis, Cambridge University, England. Data were taken from Leung et al. (1971).

Punwani, D. V., M. V. Modi, and P. B. Tarman, "A Generalized Correlation for Estimating Choking Velocity in Vertical Solids Transport," *Int. Powder Bulk Solids Handling and Processing Conf.*, Chicago, p. I11 (1976).

Rhodes, M. J., and D. Geldart, "The Hydrodynamics of Re-circulating Fluidized Beds," *Circulating Fluidized Bed Technology I*, P. Basu, ed., Pergamon Press, Oxford, p. 193 (1985).

Satija, S., J. B. Young, and L.-S. Fan, "Pressure Fluctuations and Choking Criterion for Vertical Pneumatic Conveying of Fine Particles," *Powder Technol.*, **43**, 257 (1985).

Schnitzlein, M. G., and H. Weinstein, "Flow Characterization in High-Velocity Fluidized Beds Using Pressure Fluctuations," *Chem. Eng. Sci.*, **43**, 2605 (1988).

Smith, T. N., "Limiting Volume Fractions in Vertical Pneumatic Transport," *Chem. Eng. Sci.*, **33**, 745 (1978).

Takeuchi, H., T. Hirama, and T. Chiba, "A Quantitative Definition and Flow Regime Diagram for Fast Fluidization," *Powder Technol.*, **47**, 195 (1986).

Van Swaaij, W. P. M., C. Buurman, and J. W. Van Breugel, "Shear Stress on the Wall of a Dense-Solids Riser," *Chem. Eng. Sci.*, **25**, 1818 (1970).

Weinstein, H., and J. Li, "An Evaluation of the Actual Density in the Acceleration Section of Vertical Risers," *Powder Technol.*, **57**, 77 (1989).

Wen, C. Y., and Chen, L. H., "Fluidized Bed Freeboard Phenomena: Entrainment and Elutriation," *AIChE J.*, **28**, 117 (1982).

Xu, G., K. Nomura, N. Nakagawa, and K. Kato, "Dynamics at the Transition from Dilute Transport to Dense Fluidization in Two CFBs with Different Diameters," *Fluidization '97, Science and Technology*, Y. Jin, J. Li, S. Mori, and M. Horio, eds., Tsinghua University Press, Beijing, p. 139 (1997a).

Xu, G., K. Nomura, N. Nakagawa, and K. Kato, "Accumulative Choking in Circulating Fluidized Beds," *3rd SCEJ Fluidization Symp.*, SCEJ, Tokyo, 354 (1997b).

Xu, G., and J. Li, "Analytical Solution of the Energy-Minimization

Multi-Scale Model for Gas-Solid Two-Phase Flow," *Chem. Eng. Sci*., **53**, 1349 (1998).
Xu, G., K. Nomura, N. Nakagawa, and K. Kato, "Collapse of Dilute Suspension in Different Circulating Fluidized Risers with Respect to Different Particles," *Can. J. Chem. Eng*., **77**, 238 (1999a).
Xu, G., K. Nomura, N. Nakagawa, and K. Kato, "The Saturation Carrying Capacity in Different Circulating Fluidized Beds for Different Particles," *Circulating Fluidized Bed Technology VI*, J. Werther, ed., Dechema e. V., Würzburg, p. 149 (1999b).
Xu, G., K. Nomura, N. Nakagawa, and K. Kato, "Hydrodynamic Dependence on Riser Diameter for Different Particles in Circulating Fluidized Beds," *Powder Technol*., **113**, 80 (2000).
Yang, G., and J. Sun, *Fluidization '90, Science and Technology*, M. Kwauk and M. Hasatani, eds., Science Press, Beijing, p. 37 (1990).
Yang, W., "A Mathematical Definition of Choking Phenomenon and a Mathematical Model for Predicting Choking Velocity and Choking Voidage," *AIChE J*., **21**, 1013 (1975).
Yang, W., "A Criterion for 'Fast Fluidization'," 3*rd Int. Conf. on Pneumatic Transport*, BHRA Copyright, Bedford, Paper E5 (1976).
Yang, W., "Criteria for Choking in Vertical Pneumatic Conveying Lines," *Powder Technol*., **35**, 143 (1983).
Yang, W., "Mechanistic Models for Transitions Between Regimes of Fluidization," *AIChE J*., **30**, 1025 (1984).
Yerushalmi, J., and N. T. Cankurt, "Further Studies of the Regimes of Fluidization," *Powder Technol*., **24**, 187 (1979).
Yerushalmi, J., and A. A. Avidan, *Fluidization* (2nd ed.), J. F. Davidson, R. Clift, D. Harrison, eds., Academic Press, London, p. 225 (1985).
Yousfi, Y., and G. Gau, "Aerodynamique de L'ecoulement Vertical de Suspensions Concentrees Gaz-Solides: I. Regimes D'ecoulement et Stabilite Aerodynamique," *Chem. Eng. Sci*., **29**, 1939 (1974).
Zenz, F. A., "Two-Phase Fluid-Solid Flow," *Ind. Eng. Chem*., **41**, 2801 (1949).
Zenz, F. A., and D. F. Othmer, *Fluidization and Fluid-Particle Systems*, Reinhold Publishing, New York (1960).
Zenz, F. A., and N. A. Weil, "A Theoretical-Empirical Approach to the Mechanism of Particle Entrainment from Fluidized Beds," *AIChE J*., **4**, 472 (1958).

Appendix

The compiled experimental data, compared with the calculations from the correlations with relatively higher accuracy, are summarized in Tables A1 and A2 for accumulative and classical choking, respectively.

Table A1. Literature Saturation Carrying Capacity vs. Calculations for Accumulative Choking

Set No.	Particle	D_t (mm)	U_{ck} (m/s)	$G^*_{s,exp}$ [kg/(m^2·s)]	$G^*_{s,cal}$ [kg/(m^2·s)]							
					C1	C3	C4	C10	C11	C12	C13	C14
D1	FCC-I	66	1.30	4.00	56.20	3.68	3.70	7.98	4.49	12.09	4.28	5.87
			1.60	7.50	71.27	7.53	7.51	15.18	8.10	17.75	8.01	10.22
			1.95	15.10	88.86	14.65	14.66	25.13	14.22	25.60	14.31	17.09
			2.40	26.40	111.47	28.99	28.86	40.05	25.68	37.59	25.97	29.00
			2.65	32.50	124.03	39.99	39.82	49.27	34.04	45.15	34.38	37.19
		97	1.10	2.30	46.15	1.38	1.40	3.95	2.79	8.88	3.30	4.53
			1.50	7.00	66.25	4.11	4.11	12.63	6.74	15.76	8.56	10.56
			1.85	14.50	83.84	8.35	8.35	22.13	12.24	23.22	15.91	18.29
			2.10	21.00	96.40	12.72	12.66	29.85	17.56	29.36	22.97	25.32
			2.30	26.60	106.45	17.15	17.15	36.54	22.75	34.74	29.81	31.91
		150	1.10	4.25	46.15	0.89	0.86	3.95	2.79	8.88	4.43	5.71
			1.30	6.85	56.20	1.62	1.60	7.98	4.49	12.09	7.44	9.05
			1.60	13.30	71.27	3.31	3.29	15.18	8.10	17.75	13.92	15.76
			1.90	22.50	86.35	5.90	5.87	23.61	13.21	24.40	23.06	24.66
	FCC-II	97	1.12	5.00	45.19	1.61	1.64	6.44	3.96	9.05	5.01	5.81
			1.43	9.46	59.20	3.64	3.67	13.59	7.94	14.23	10.28	10.95
			1.55	13.70	64.62	4.74	4.78	16.75	9.98	16.51	12.97	13.45
			1.78	14.90	75.02	7.42	7.33	23.35	14.80	21.33	19.28	19.08
			2.20	27.00	94.00	14.63	14.59	37.10	27.04	31.57	35.10	32.38
	Alumina	97	1.90	6.50	54.10	3.40	3.43	12.71	4.11	22.74	6.74	7.03
			2.10	9.50	62.15	5.19	5.17	17.11	5.46	27.37	9.12	9.42
			2.40	12.70	74.23	8.90	8.81	24.41	7.99	35.04	13.45	13.70
			2.60	15.80	82.28	12.16	12.05	29.69	10.03	40.63	16.83	17.02
			3.12	21.80	103.21	24.16	23.96	44.90	16.85	56.93	27.58	27.42
			3.17	22.20	105.22	25.61	25.48	46.46	17.63	58.62	28.76	28.55
	Alumina	150	1.25	1.20	27.94	0.29	0.30	1.32	1.25	10.48	1.27	1.42
			1.40	1.80	33.98	0.53	0.56	3.52	1.72	12.93	1.96	2.16
			1.60	3.13	42.03	1.02	1.02	6.86	2.52	16.55	3.13	3.40
			1.90	5.26	54.10	2.20	2.16	12.71	4.11	22.74	5.44	5.80
			2.10	7.83	62.15	3.35	3.34	17.11	5.46	27.37	7.37	7.78

Table continued

Table A1. (Continued) Literature Saturation Carrying Capacity vs. Calculations for Accumulative Choking

Set No.	Particle	D_t (mm)	U_{ck} (m/s)	$G^*_{s,exp}$ [kg/(m^2·s)]	$G^*_{s,cal}$ [kg/(m^2·s)]							
					C1	C3	C4	C10	C11	C12	C13	C14
D1	Sand	66	1.80	7.30	55.52	1.72	1.74	3.62	2.60	22.68	7.50	5.67
			2.50	19.00	103.63	11.85	11.78	19.43	6.63	41.64	18.01	16.63
			3.00	27.80	138.00	28.49	28.27	33.70	11.13	58.34	26.80	27.11
			3.20	30.60	151.74	38.09	38.04	40.02	13.38	65.74	30.56	31.85
			3.50	36.00	172.36	56.22	56.00	50.11	17.26	77.59	36.44	39.55
		97	2.45	11.60	100.19	7.25	7.28	18.13	6.26	40.11	11.77	11.31
			2.60	13.10	110.50	9.79	9.77	22.10	7.41	44.77	13.48	13.38
			3.10	18.30	144.87	22.42	22.25	36.82	12.22	61.99	19.63	21.22
			3.35	22.10	162.05	31.55	31.33	44.97	15.24	71.55	22.92	25.67
			3.65	26.30	182.67	45.46	45.15	55.42	19.45	83.86	27.04	31.45
			3.80	28.70	192.98	53.73	53.49	60.89	21.81	90.34	29.16	34.51
			4.10	32.80	213.60	73.18	72.94	72.33	27.07	103.98	33.54	40.99
			4.48	38.90	239.72	103.95	103.66	87.70	34.84	122.51	39.31	49.81
		150	1.90	3.70	62.39	1.08	1.13	5.55	3.04	25.06	3.95	3.45
			2.10	5.00	76.14	2.01	1.97	9.74	4.04	30.16	5.22	4.87
			2.30	6.80	89.88	3.35	3.38	14.38	5.23	35.69	6.59	6.48
			2.50	8.90	103.63	5.19	5.12	19.43	6.63	41.64	8.03	8.27
D2	HFZ-20	152	1.00	4.90	40.34	0.74	0.75	4.83	3.33	7.36	7.53	7.59
			1.34	10.00	55.60	1.95	1.92	12.41	7.65	12.64	17.71	16.13
			1.65	17.00	69.52	3.82	3.77	20.90	13.82	18.58	32.11	27.26
			2.16	40.00	92.42	8.99	9.03	37.62	29.74	30.58	68.52	53.19
	FCC	152	0.94	4.00	28.54	0.48	0.48	4.91	2.96	6.19	6.53	6.11
			1.13	7.00	34.83	0.88	0.86	8.63	4.99	8.70	11.12	9.77
			1.30	15.00	40.47	1.38	1.39	12.45	7.44	11.28	16.58	13.90
D3	HA54	100	0.99	7.00	22.22	0.71	0.72	8.24	5.38	6.43	10.46	7.51
			1.16	10.00	26.17	1.16	1.16	11.90	8.45	8.62	16.20	11.04
			1.53	17.00	34.76	2.72	2.71	21.24	18.57	14.38	34.64	21.53
D4	FCC	100	1.30	11.00	30.79	1.62	1.61	12.22	6.79	10.66	7.40	6.88
			1.50	14.50	35.81	2.55	2.51	16.87	10.20	13.90	11.07	9.81
			1.75	28.00	42.08	4.14	4.11	23.32	15.81	18.48	17.02	14.34
D5	FCC	50	0.80	1.50	21.60	0.73	0.74	1.85	1.40	4.50	0.73	1.06
			0.95	2.50	26.24	1.31	1.32	4.12	2.28	6.19	1.22	1.67
			1.05	5.00	29.34	1.83	1.82	5.85	3.03	7.45	1.65	2.17
			1.10	7.00	30.89	2.14	2.10	6.77	3.46	8.12	1.89	2.45
	Sand	50	2.50	30.00	150.72	36.20	36.09	28.53	12.62	43.59	25.58	26.13
D6	Plastic	200	4.22	9.63	123.13	15.77	5.38	9.94	6.56	22.46	10.01	10.81
			5.15	19.56	164.48	38.16	13.02	19.75	11.54	32.43	18.98	20.00
			5.87	30.33	196.63	65.74	22.56	28.56	16.75	41.32	28.13	29.20
			6.39	41.53	219.60	92.01	31.71	35.42	21.27	48.28	35.87	36.89
			7.42	67.16	265.53	163.99	56.31	50.48	32.55	63.66	54.44	55.11
	Steel	200	3.36	27.91	591.28	67.33	79.54	89.62	54.67	123.68	54.39	58.81
			3.75	39.03	679.70	102.72	122.48	116.95	74.47	151.22	74.20	79.15
			4.39	72.84	826.22	185.46	221.46	167.05	116.57	202.37	114.60	119.91
			4.63	81.06	881.80	225.87	268.21	187.52	135.86	223.55	132.46	137.71
D7	FCC	76	4.70	207.87	222.75	208.26	207.59	140.63	155.87	129.65	172.18	159.60
			5.85	410.00	279.71	413.73	412.18	205.45	290.54	194.36	312.13	270.76
			6.00	285.00	287.14	447.73	445.80	214.47	312.24	203.68	334.25	287.75
			6.10	307.00	292.10	471.44	469.68	220.54	327.27	210.01	349.52	299.40
			6.37	460.00	305.47	539.53	537.27	237.22	370.19	227.53	392.87	332.18
			6.88	470.00	330.63	684.88	681.91	269.62	460.50	262.23	483.09	399.17
			6.52	465.00	312.65	578.68	576.07	246.34	394.67	237.20	417.45	350.59
			7.39	600.00	356.00	855.63	851.97	303.56	564.86	299.48	585.92	473.85
D8	FCC	54	0.68	0.95	17.19	0.24	0.22	0.96	1.05	3.30	0.96	1.20
			0.96	2.65	25.24	0.75	0.77	5.14	2.79	6.25	2.68	2.96
			1.51	9.75	41.07	3.24	3.20	16.93	10.12	14.44	9.81	9.30
			2.14	25.64	59.20	9.73	9.67	34.93	27.28	27.53	26.00	21.95
			2.56	42.10	71.29	17.00	16.91	49.08	45.42	38.34	42.66	33.95
D9	FCC	100	1.36	5.30	37.00	2.08	2.08	12.79	6.91	11.90	7.96	7.86
			1.47	7.80	40.20	2.67	2.66	15.37	8.62	13.74	9.92	9.55
			1.87	21.00	51.84	5.74	5.68	25.95	17.10	21.45	19.53	17.35
			2.25	36.00	62.90	10.27	10.27	37.55	28.94	30.21	32.67	27.31
			2.56	45.50	71.92	15.36	15.33	48.00	41.79	38.35	46.67	37.40
			2.74	63.00	77.16	18.98	18.91	54.44	50.70	43.49	56.27	44.10
			2.95	79.40	83.27	23.86	23.75	62.27	62.55	49.86	68.91	52.74

Table A1. (Continued) Literature Saturation Carrying Capacity vs. Calculations for Accumulative Choking

Set No.	Particle	D_t (mm)	U_{ck} (m/s)	$G^*_{s,exp}$ [kg/(m^2·s)]	$G^*_{s,cal}$ [kg/(m^2·s)]							
					C1	C3	C4	C10	C11	C12	C13	C14
D10	Gel-I	30	2.00	15.00	38.13	10.52	10.51	15.71	4.33	22.67	12.46	11.97
			2.22	23.00	43.54	15.74	15.68	20.28	5.82	27.49	16.76	15.88
			2.70	40.00	55.34	32.58	32.41	31.44	10.16	39.49	28.63	26.48
			3.50	50.00	75.00	81.96	81.57	53.26	21.26	63.83	56.40	50.57
			3.95	58.00	86.07	124.42	123.82	67.09	29.99	79.83	76.62	67.75
			2.44	34.00	48.95	22.45	22.38	25.20	7.62	32.74	21.77	20.39
			2.93	43.60	60.99	43.76	43.63	37.32	12.82	45.94	35.57	32.57
			3.16	46.00	66.65	57.27	57.08	43.53	15.90	52.83	43.34	39.34
			4.39	60.00	96.88	178.17	177.36	81.58	40.51	97.06	99.73	87.12
	Gel-II	30	2.47	52.00	34.27	7.36	7.31	20.33	2.85	32.71	85.90	50.90
			3.15	67.00	50.98	25.05	24.95	35.60	5.68	51.29	60.84	63.15
			3.89	80.00	69.17	64.02	63.69	55.10	10.36	75.78	46.75	74.45
			5.81	94.00	116.37	316.65	315.34	117.07	32.44	159.18	29.91	98.46
			2.74	64.50	40.90	12.71	12.65	26.07	3.82	39.63	73.64	56.04
			2.90	64.50	44.84	16.87	16.76	29.67	4.49	44.01	68.00	58.91
			3.40	71.80	57.13	35.54	35.40	41.88	7.06	59.07	55.14	67.16
			3.65	70.00	63.27	48.67	48.45	48.47	8.64	67.36	50.49	70.96
			4.42	83.60	82.20	108.81	108.34	70.67	14.90	95.98	40.30	81.70
			4.87	83.60	93.26	160.40	159.74	84.85	19.64	114.84	36.16	87.43
			5.33	89.00	104.57	228.01	226.96	100.20	25.38	135.71	32.78	92.97
			6.28	95.70	127.92	423.34	421.40	134.40	40.48	183.82	27.58	103.58
			6.81	100.00	140.95	569.67	567.15	154.83	50.97	213.54	25.38	109.10
	Mo-Cat.	30	2.22	33.00	90.01	39.98	39.75	28.83	13.98	31.71	13.60	18.95
			1.98	29.00	78.96	26.91	26.73	21.89	10.09	25.66	9.71	14.02
			2.43	51.50	99.68	54.40	54.16	35.38	18.07	37.48	17.68	23.97
			3.00	65.00	125.92	110.24	109.71	55.22	32.92	55.34	32.24	41.05
			3.50	71.00	148.94	183.11	182.18	74.85	51.04	73.60	49.62	60.41
			3.98	72.50	171.03	278.16	277.07	95.44	73.57	93.36	70.78	83.03
			4.37	72.00	188.99	376.10	374.54	113.34	95.98	110.99	91.45	104.44
			4.78	72.00	207.86	501.44	499.25	133.19	123.88	131.01	116.76	129.99
D11	FCC	66	3.00	44.00	141.62	59.61	59.47	63.18	48.44	56.80	48.72	50.66
			3.00	53.00	141.62	59.61	59.47	63.18	48.44	56.80	48.72	50.66
	FCC	97	1.50	10.70	66.25	4.11	4.11	12.63	6.74	15.76	8.56	10.56
			2.00	24.20	91.37	10.91	10.73	26.67	15.28	26.83	19.95	22.35
			3.00	57.30	141.62	40.50	40.36	63.18	48.44	56.80	63.14	62.08
			3.00	36.30	141.62	40.50	40.36	63.18	48.44	56.80	63.14	62.08
			3.00	62.00	141.62	40.50	40.36	63.18	48.44	56.80	63.14	62.08
			4.00	75.00	191.87	101.03	100.45	108.66	109.82	96.72	140.18	125.92
			4.00	84.00	191.87	101.03	100.45	108.66	109.82	96.72	140.18	125.92
	FCC	150	2.00	27.50	91.37	6.93	6.93	26.67	15.28	26.83	26.76	28.14
			3.00	53.00	141.62	26.21	25.93	63.18	48.44	56.80	84.68	78.14
			3.00	67.20	141.62	26.21	25.93	63.18	48.44	56.80	84.68	78.14
D12	Phos.-I	55	1.06	1.35	26.39	0.15	0.17	−5.41	0.91	8.84	0.58	0.65
			1.12	1.52	31.13	0.26	0.26	−4.75	1.07	9.79	0.85	0.93
			1.17	2.02	35.07	0.38	0.36	−4.14	1.21	10.61	1.10	1.20
			1.27	2.90	42.97	0.71	0.69	−2.80	1.53	12.35	1.73	1.86
			1.37	3.58	50.86	1.21	1.21	−1.29	1.90	14.21	2.50	2.67
			1.47	4.55	58.76	1.90	1.86	0.38	2.32	16.19	3.42	3.64
			1.55	5.55	65.07	2.60	2.56	1.83	2.70	17.86	4.27	4.52
	Phos.-II	55	1.47	2.02	5.31	0.00	0.00	−5.84	1.08	15.90	50.82	0.63
			1.49	2.40	6.89	0.00	0.00	−5.60	1.12	16.30	51.90	1.15
			1.54	3.03	10.84	0.00	0.01	−4.97	1.23	17.33	53.28	2.44
			1.58	3.75	13.99	0.01	0.01	−4.44	1.32	18.17	53.94	3.47
			1.62	4.60	17.15	0.03	0.03	−3.89	1.42	19.03	54.43	4.50
			1.68	5.64	21.89	0.07	0.05	−3.03	1.57	20.36	54.99	6.03
D13	Sand-I	107	2.00	5.01	77.39	2.43	2.45	7.49	3.82	28.13	6.22	5.64
			2.20	7.66	92.54	4.21	4.19	12.07	5.01	33.56	8.20	7.77
			2.28	8.90	98.22	5.06	5.02	13.90	5.51	35.71	8.98	8.65
			2.42	10.05	109.20	7.01	6.98	17.62	6.57	40.03	10.57	10.45
			2.80	15.43	137.97	14.35	14.38	28.36	9.95	52.43	15.11	15.84
			3.10	31.71	160.69	22.85	22.79	37.80	13.30	63.29	19.05	20.75
	FCC	107	1.20	2.18	74.35	2.01	1.96	2.29	3.26	11.41	4.14	6.32
			1.24	5.32	77.58	2.29	2.35	3.10	3.58	12.12	4.63	6.97
			1.27	7.07	80.00	2.51	2.43	3.73	3.83	12.67	5.01	7.49

Table A2. Literature Critical Solid Flow Rate Compared with Calculations for Classical Choking

Set No.	Particle	D_t (mm)	U_{ck} (m/s)	$G^*_{s,exp}$ [kg/(m^2·s)]	$G^*_{s,cal}$ [kg/(m^2·s)]					
					C1	C2	C7	C8	C9	C12
D14	Salt	45	1.75	11.19	51.47	10.09	13.67	2.59	11.03	21.29
			2.38	40.32	92.43	41.16	78.45	21.41	63.13	37.61
			2.93	69.09	128.18	106.48	210.90	88.64	129.44	55.25
	GBs	45	3.41	32.53	−59.11	40.41	−13.49	18.73	14.39	72.26
			3.96	84.67	−16.83	80.04	−0.81	52.25	54.03	95.29
			4.57	145.26	30.06	154.09	0.38	139.08	110.13	124.21
			6.16	315.34	152.29	603.28	159.96	1025.37	316.30	215.79
D15	GBs-I	32	1.22	9.91	84.83	11.67	38.02	4.10	31.65	11.86
			1.31	19.69	91.75	16.16	48.17	6.68	41.73	13.52
			1.68	43.95	120.19	50.37	108.85	36.78	94.36	21.43
			1.77	63.07	127.11	63.95	128.89	52.50	109.88	23.60
			2.01	92.37	145.56	114.36	194.06	124.31	156.48	29.86
			2.10	111.98	152.48	139.71	223.25	166.82	175.90	32.38
	GBs-II	32	1.58	9.91	78.83	12.60	29.74	4.10	18.07	18.52
			1.71	19.59	88.82	18.08	42.92	7.07	28.80	21.44
			1.74	36.50	91.13	19.58	46.42	7.96	31.47	22.14
			1.74	46.18	91.13	19.58	46.42	7.96	31.47	22.14
			2.13	73.00	121.11	49.35	111.15	31.89	73.05	32.19
			2.13	102.05	121.11	49.35	111.15	31.89	73.05	32.19
			2.29	129.36	133.41	68.71	149.57	52.33	93.76	36.81
			2.44	146.00	144.94	91.83	192.89	80.65	115.11	41.39
			2.44	159.66	144.94	91.83	192.89	80.65	115.11	41.39
	GBs-II	32	2.32	9.09	15.25	19.28	0.07	7.82	7.88	36.37
			2.50	24.06	29.09	27.13	0.88	13.07	19.67	41.76
			2.53	58.60	31.40	28.65	1.18	14.18	21.79	42.69
			2.71	92.37	45.23	39.22	4.23	22.73	35.45	48.48
			2.83	102.05	54.46	47.82	7.91	30.60	45.46	52.53
			2.96	130.85	64.45	58.71	13.90	41.63	57.10	57.08
D16	Sand-I	25	2.09	51.05	110.37	36.24	77.99	23.01	48.56	31.29
			2.36	102.11	132.60	63.15	137.60	52.87	79.03	39.18
			3.51	205.81	227.27	387.70	728.38	753.12	270.78	81.65
	Sand-II	25	2.70	91.47	139.30	86.77	160.64	85.17	95.22	49.85
			3.20	137.74	180.46	188.66	360.78	268.76	167.01	68.26
	Sand-III	25	2.31	27.65	51.37	25.37	6.36	13.55	18.33	36.83
			2.87	103.70	97.47	68.44	51.28	60.03	67.33	55.04
			3.17	207.40	122.17	107.82	105.99	118.25	100.74	66.15
			3.46	358.97	146.04	160.87	188.06	213.97	137.77	77.78
	Sand-IV	25	2.79	69.67	58.27	48.66	9.24	36.07	42.31	51.93
			3.17	101.31	89.55	87.23	38.17	86.40	78.85	65.77
			3.51	203.41	117.54	138.97	93.08	172.74	117.80	79.41
D17	Sand	20	2.70	71.70	95.30	56.47	66.52	58.09	58.80	49.14
			2.93	104.70	113.96	82.06	118.28	101.44	83.14	57.16
			3.32	157.70	145.27	144.49	258.47	234.44	130.82	71.87
			3.99	283.20	200.18	337.81	725.84	799.26	235.10	101.34
			4.60	387.20	249.58	646.38	1470.08	1930.63	351.37	131.78
D18	FCC	76	2.41	207.87	109.31	122.60	219.49	95.04	182.05	37.68
			3.11	285.00	143.98	393.31	504.90	506.19	342.48	60.39
			2.78	320.00	127.64	235.52	350.90	245.99	260.81	49.08
			3.16	395.00	146.46	423.05	531.52	559.32	355.79	62.20
			2.90	410.00	133.58	285.71	402.49	323.97	289.27	53.07
			3.00	460.00	138.54	333.61	449.19	402.90	314.06	56.50
			3.23	470.00	149.93	467.62	570.41	640.60	374.84	64.77

Manuscript received July 5, 2000, and revision received Jan. 2, 2001.